EGCG suppresses nasopharyngeal carcinoma progression by reducing *PACRG* methylation via inhibition of DNA methyltransferases

Ruizhen Wu¹, Jun Jiang², Jianhong Ma^{1*}

¹Department of Nutrition, Eye & ENT Hospital, Fudan University, Shanghai, China ²State Key Laboratory of Genetic Engineering, Shanghai Engineering Research Center of Industrial Microorganisms, School of Life Sciences, Fudan University, Shanghai, China

Submitted: 29 May 2025; Accepted: 22 August 2025 Online publication: 28 October 2025

Arch Med Sci DOI: https://doi.org/10.5114/aoms/209819 Copyright © 2025 Termedia & Banach

Abstract

Introduction: Nasopharyngeal carcinoma (NPC) is a serious cancer with a poor prognosis and a significant risk of metastasis. Although its epigenetic control mechanisms are still unknown, epigallocatechin-3-gallate (EGCG) exhibits strong anticancer properties. Promoter methylation in malignancies often silences *PACRG*, a putative tumor suppressor gene. This study aimed to determine whether EGCG suppresses cancer by altering *PACRG* gene expression in NPC cells.

Material and methods: NPC cells were subjected to EGCG or 5-aza-dC. Cellular functions were assessed by CCK-8, Transwell, and flow cytometry assays. Methylation-specific PCR (MSP) was used to identify *PACRG* promoter methylation, and gene expression was measured using quantitative real-time PCR (qRT-PCR) and Western blot (WB). The expression of DNA methyltransferase-related genes was evaluated. siRNA targeting *PACRG* was used to assess its functional involvement in the effects mediated by EGCG.

Results: EGCG exerted dose- and time-dependent effects on NPC cells by reducing proliferation and migration while inducing apoptosis and G2 phase cell cycle arrest. Mechanistically, EGCG significantly reduced the mRNA expression and enzymatic activity of *DNMT1*, *DNMT3A*, and *DNMT3B*, resulting in decreased *PACRG* promoter methylation and restored *PACRG* expression. Functional assays revealed that knockdown of PACRG diminished the inhibitory effect of EGCG on NPC cells, indicating that the epigenetic reactivation of PACRG partially mediates the tumor-suppressive function of EGCG.

Conclusions: Our results revealed that EGCG inhibits NPC progression by reducing *PACRG* promoter methylation, highlighting that *PACRG* demethylation and reactivation are a promising therapeutic strategy.

Key words: epigallocatechin-3-gallate, nasopharyngeal carcinoma, *PACRG*, methylation.

Introduction

A malignant tumor that develops from the nasopharyngeal mucosa's epithelial cells, nasopharyngeal carcinoma (NPC) has a specific geographic distribution and is most common in Southeast Asia and southern China [1]. Numerous variables, including genetic predisposition, environmental toxins, dietary practices, and Epstein-Barr virus infection, all contribute to

*Corresponding author: Jianhong Ma MD Department of Nutrition Eye & ENT Hospital Fudan University Shanghai, 200031, China E-mail: jeepdo@126.com its etiology [2, 3]. Despite advances in radiotherapy, chemotherapy, and immunotherapy, NPC remains associated with high morbidity and mortality, mainly due to late diagnosis and treatment resistance [4–6]. Recent efforts have focused on exploring novel treatment strategies and molecular targets.

Epigallocatechin-3-gallate (EGCG), a primary polyphenol in green tea, has shown anticancer effects by modulating oxidative stress, apoptosis, and autophagy pathways [7–9]. In NPC, EGCG has been reported to suppress proliferation, migration, and stemness via mechanisms that include the inactivation of NF- κ B and modulation of adhesion molecules [10–12]. Notably, EGCG can influence DNA methylation, thereby restoring the expression of tumor suppressor genes and enhancing the efficacy of chemotherapeutic agents [13–16]. However, its epigenetic mechanisms in NPC remain incompletely understood.

PACRG (Parkin co-regulated gene) has been identified as a tumor suppressor in various cancers and is subject to epigenetic silencing through promoter hypermethylation [17–20]. In NPC, aberrant methylation of PACRG has been observed [18], yet its functional relevance remains largely unexplored. Given the emerging role of EGCG in modulating gene methylation, it is plausible that EGCG may exert its antitumor effects by epigenetically reactivating the *PACRG* gene.

In this study, we investigated whether EGCG suppresses NPC progression by demethylating and upregulating PACRG, thereby inhibiting tumor cell proliferation and invasion. This work provides insights into the epigenetic mechanisms of EGCG and highlights PACRG as a potential therapeutic target in NPC.

Material and methods

Microarray data analysis

The GSE12452 and GSE64634 datasets originated from the Gene Expression Omnibus (GEO, https://www.ncbi.nlm.nih.gov/gds/). GSE12452 comprises 31 NPC samples and 10 matching controls, while GSE64634 comprises 12 NPC samples and 4 matching controls. Up-regulated differentially expressed GEO2R defined genes (DEGs) with a fold change (FC) threshold > 2, and down-regulated DEGs as those with an FC < 0.5, and the p-value threshold was < 0.05. These cutoff values were selected based on previously published studies of nasopharyngeal carcinoma using GEO datasets, such as Zhang $et\ al.$, which employed the same thresholds to identify robust and biologically relevant DEGs [21].

Identification and enrichment analysis of overlapping DEGs

The Venn diagram (https://bioinformatics.psb. ugent.be/webtools/Venn/) web tool was applied to

conduct an intersection analysis of downregulated and upregulated DEGs from the GSE12452 and GSE64634 datasets, identifying overlapping DEGs. Gene Ontology (GO) and Kyoto Encyclopedia of Genes and Genomes (KEGG) enrichment analyses were then conducted on these overlapping DEGs using DAVID (https://david.ncifcrf.gov/).

Identification and expression analysis of key genes

Protein-protein interaction (PPI) network analysis among the overlapping DEGs was conducted using the Search Tool for Interacting Genes/Proteins (STRING, https://string-db.org/). The constructed PPI network was further analyzed using Molecular Complex Detection (MCODE) and Maximal Clique Centrality (MCC) algorithms by Cytoscape (version 3.7.1). Key genes were identified by intersecting the results of both algorithms. To evaluate the expression levels of the identified key genes, boxplot visualization and data processing were performed with R. The GSE12452 and GSE64634 datasets were used to compare the expression levels of these genes between the tumor and normal groups.

Cell culture

The nasopharyngeal epithelial NP69 cell line and the human nasopharyngeal carcinoma (NPC) cell lines HK-1 and C666-1 were purchased from Yaji Biological Technology Co., Ltd. (Shanghai, China). Under standard culture conditions, NP69 cells were cultured in KM medium (2101; Yaji Biological Technology Co., Ltd., Shanghai, China), a specifically formulated medium for epithelial cell growth. The HK-1 and C666-1 cells were kept in RPMI-1640 medium (C22400500BT; Gibco, USA) with 1% penicillin-streptomycin (15140122; Gibco, USA) and 10% FBS (10091148; Gibco, USA) added as supplements. At 37°C, the cells were cultured in a humidified environment with 5% CO₂.

Cell treatment

HK-1 and C666-1 cells were planted in 6-well plates at the appropriate density and exposed to EGCG (E4143; Sigma-Aldrich, USA), which was dissolved in distilled water at a stock concentration of 100 μ M and stored at –20°C until use. Final concentrations of 0, 10, 20, and 40 μ M EGCG were applied for 24, 48, and 72 h. A distilled water vehicle control was included to match the solvent volume used in the EGCG-treated groups. This time window is based on two studies by Wang et al. [10] and He et al. [13], which demonstrated that a 24–72-hour period is sufficient to induce EGCG-mediated epigenetic changes. In parallel, the cells were treated with 5 μ M 5-aza-2'-deox-

ycytidine (5-aza-dC; A3656; Sigma-Aldrich, USA), a DNA methyltransferase inhibitor, for 48 h.

Cell transfection

For transient transfection, NPC cells were cultivated until confluence was approximately 70–80%. siRNA targeting *PACRG* (si-*PACRG*-1 and si-*PACRG*-2) was used to inhibit *PACRG* expression at a final concentration of 50 nM. Non-targeting siRNA (si-NC) was used as a negative control. The reagent Lipofectamine 3000 (L3000015; Thermo Fisher Scientific, USA) was used according to the manufacturer's guidelines.

Quantitative real-time PCR (qRT-PCR)

According to the manufacturer's instructions, 1 µg of RNA was reverse-transcribed into cDNA using the PrimeScript RT reagent Kit (RR047A; Takara, Japan). SYBR Green PCR Master Mix (RR420Q; Takara, Japan) was employed to conduct qRT-PCR via the StepOnePlus Real-Time PCR System (Applied Biosystems, USA). Gene expression levels were analyzed via the 2^{-ΔΔCT} method with GAPDH normalization. Table I presents the primer sequences used for qRT-PCR.

Western blot (WB) assay

RIPA lysis buffer (R0020; Solarbio, Beijing, China) containing phosphatase and protease inhibitors (P1046; Beyotime, China) was employed to obtain NPC cell protein lysates. The protein concentration was detected using the BCA Protein Assay Kit (P0012; Beyotime, China). After being separated by 10% SDS-PAGE, proteins in comparable amounts were transferred onto PVDF membranes (FFP28; Beyotime, China). Primary antibodies used in this research included anti-PACRG (SAB1410229, 1:1000; Sigma-Aldrich, USA) and anti-GAPDH (ab181602, 1:10000; Abcam, China), the latter serving as an internal loading control. A ChemiDoc imaging system (Bio-Rad, Shanghai, China) was used to capture

the protein bands, and a Genomic DNA Extraction kit (DP304; Tiangen, Beijing, China) was employed to visualize the bands. Image J software (NIH, USA) was used to assess the intensity of each band.

Dot blot assay

Genomic DNA was extracted from HK-1 and C666-1 cells using the TIANamp Genomic DNA Kit (TIANGEN, China), quantified using a NanoDrop spectrophotometer, and denatured at 95°C for 10 min. DNA samples (50, 100, and 200 ng) were spotted onto a positively charged nylon membrane (41105339; Sigma-Aldrich, USA), air-dried, and cross-linked by UV irradiation. After blocking with 5% non-fat milk in TBST for 1 h at room temperature, the membrane was incubated overnight at 4°C with anti-5hmC antibody (39769, 1:10,000; Active Motif, USA) or anti-5mC antibody (28692, 1: 10,000; Cell Signaling Technology, USA). After TBST washing, the membrane was incubated with HRP-conjugated secondary antibody (SA00001-2, 1:10000; Proteintech, USA) for 1 h at room temperature. Signal detection was performed using an ECL system (Millipore), and dot intensity was analyzed with ImageJ software.

Cell Counting Kit-8 (CCK-8) assay

Cell viability was assessed using the CCK-8 (KGA9310; KeyGEN, Nanjing, China) according to the manufacturer's guidelines. NPC cells were seeded at a density of 5×10^3 cells per well in 96-well plates. After treatment with various concentrations of EGCG, 5-aza-dC, or siRNA as indicated, $10 \, \mu l$ of CCK-8 reagent was applied to every well at the specified time points (24, 48, 72 h or days 1, 3, 5, 7). Absorbance was measured using a microplate reader (Kehua, Shanghai, China) at 450 nm.

Flow cytometry

For apoptosis analysis, NPC cells were separated by trypsin-EDTA (15400054; Thermo Fisher

Table I. Primer sequences for qRT-PCR

Target	Direction	Sequence (5'-3')
PACRG	Forward	GGAGGAGTTTCTGTGGAGCC
PACRG	Reverse	TACGGATGTGAGCAGGAGGT
DNMT1	Forward	AGGAGGGCTACCTGGCTAAA
DNMT1	Reverse	GCATCTGCCATTCCCACTCT
DNMT3a	Forward	CGAGTTCTGGAGATGCTGACTT
DNMT3a	Reverse	TTCTTCTCAGCCACTGCCCG
DNMT3b	Forward	CCGCTTCCTCGCAGCAG
DNMT3b	Reverse	CGATCGCCGAGCTAGGTTTA
GAPDH	Forward	AATGGGCAGCCGTTAGGAAA
GAPDH	Reverse	GCGCCCAATACGACCAAATC

Scientific, USA) and stained with propidium iodide (PI) and Annexin V using a commercial apoptosis detection kit (88-8007-74; Thermo Fisher Scientific, USA), following the manufacturer's directions. Flow cytometry was performed using a flow cytometer (Jiyuan, Guangzhou, China), and the data were analyzed with FlowJo software (FlowJo, Hangzhou, China). We calculated the proportions of necrotic, late apoptotic, and early apoptotic cells.

For cell cycle analysis, NPC cells were fixed in 5 ml of cold 70–80% ethanol and stored overnight in the dark at 4°C. The cells were washed with PBS and then exposed to 0.5 ml of propidium iodide/RNase buffer for 15 min at 25°C under light-protected conditions. Flow cytometry was used to examine cell distribution in the G1, S, and G2 phases, including calculation of the percentage of cells in each phase.

Cell migration assays

Cell migration was assessed using a Transwell assay. Transfected NPC cells were seeded in serum-free medium in the upper chamber, while the lower chamber contained 10% FBS as a chemoattractant. After incubation, migrated cells were fixed with 4% paraformaldehyde, stained with DAPI, and quantified under an inverted microscope.

Methylation-specific PCR (MSP)

Genomic DNA was extracted using the TIANamp Genomic DNA Kit (Tiangen, China), and its purity was assessed with a NanoDrop microspectrophotometer (Thermo, China) according to the manufacturer's instructions. Bisulfite modification of the purified DNA was conducted with the EZ DNA Methylation-Gold Kit (D5005; Zymo Research, USA). The methylated specific upstream primer of PACRG was 5'-GTATAGTTTCGTTTTTC-GTGGAC-3'; the methylated specific downstream primer of PACRG was 5'-CTAAAAAATCGTAATTCTA-ACGCGTA-3'; the unmethylated specific upstream primer of PACRG was 5'-GTATAGTTTTTGT-GATGT-3'; and the unmethylated specific downstream primer of PACRG was 5'-CTAAAAAATCATA-ATTCTAACACATA-3'. ABL1 was used as an internal control for DNA integrity. The forward primer was 5'-AGCATCTGACTTTGAGCC-3', and the reverse primer was 5'-CCCATTGTGATTATAGCCTAAGAC-3'.

DNMT activity assay

The DNMT enzyme activity was measured using the EpiQuik DNA Methyltransferase Activity/Inhibition Assay Kit (P-3001; EpigenTek, NY, USA). In brief, nuclear proteins were extracted from NPC cells treated with EGCG or 5-aza-dC, and the methyltransferase reaction was performed in a microplate with pre-coated substrate DNA, following the kit instructions. The catalytic products

were measured by absorbance at 450 nm, which reflects the enzyme activity level of DNMT.

Statistical analysis

Statistical analyses were performed using R software. All experiments were conducted with biological replicates, and each experiment was independently repeated on at least three separate days to ensure reproducibility. Data are expressed as mean ± standard deviation (SD). For comparisons among multiple groups, one-way ANOVA was used, followed by Tukey's post hoc test to correct for multiple comparisons. When data did not meet the assumptions of normality or homogeneity of variance (assessed by Shapiro-Wilk and Levene's tests), non-parametric alternatives such as the Kruskal-Wallis test with Dunn's post hoc correction were applied. For two-group comparisons, unpaired twotailed Student's t-tests were used, or Mann-Whitney U tests if normality was not assumed. A p-value < 0.05 was considered statistically significant.

Results

EGCG inhibits the cell function of NPC cells in a dose- and time-dependent manner

The cell viability of NPC cell lines was assessed using the CCK-8 assay after being subjected to different levels of EGCG (0, 10, 20, 40 µM). The results demonstrated a dose-dependent decline in cell viability with increasing EGCG concentrations (Figures 1 A, B). The impact of different treatment durations (0, 24, 48, and 72 h) with 40 µM EGCG was evaluated. A time-dependent decrease in cell viability was observed in both NPC cell lines (Figures 1 C, D). Furthermore, the impact of EGCG on cell proliferation was assessed over a range of concentrations (0, 10, 20, 40 μ M) for various periods (1, 3, 5, and 7 days). The outcomes showed that the proliferation of NPC cells decreased with increasing EGCG concentrations at each time point. Additionally, cell proliferation decreased at the same EGCG concentration as the treatment duration increased (Figures 1 E, F). In the cell migration assay, EGCG treatment was associated with a significant, dose-dependent decrease in the number of migratory cells in NPC cell lines at each time point. Quantitative analysis revealed that 20 µM and 40 µM EGCG significantly inhibited cell migration compared to the untreated control group (Figures 2 A, B). These outcomes imply that EGCG can efficiently and dose-dependently inhibit NPC cell migration.

EGCG induces apoptosis and G2 arrest in NPC cells

NPC cells were subjected to varying concentrations of EGCG (0, 10, 20, and 40 μ M) for 48

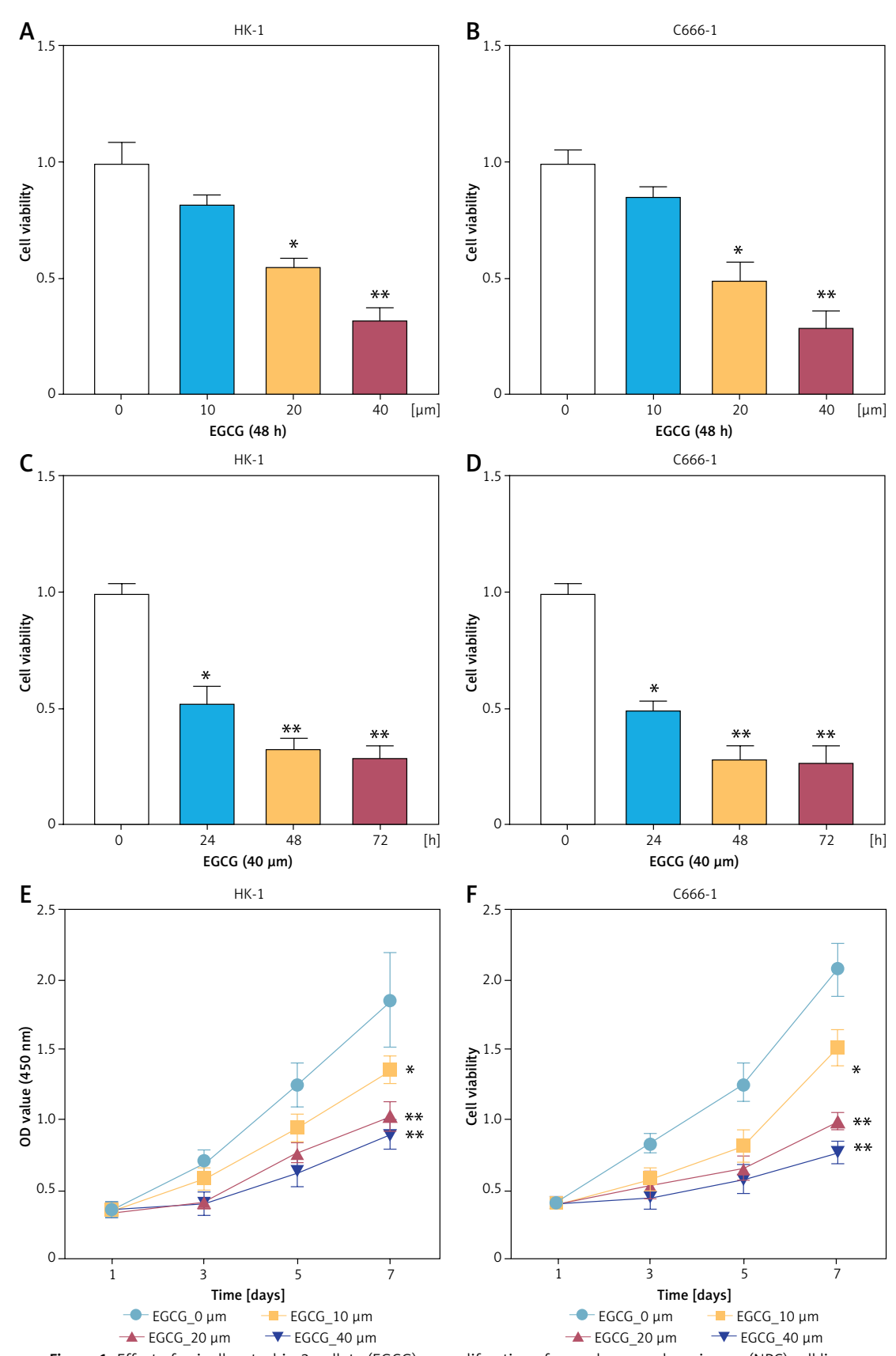
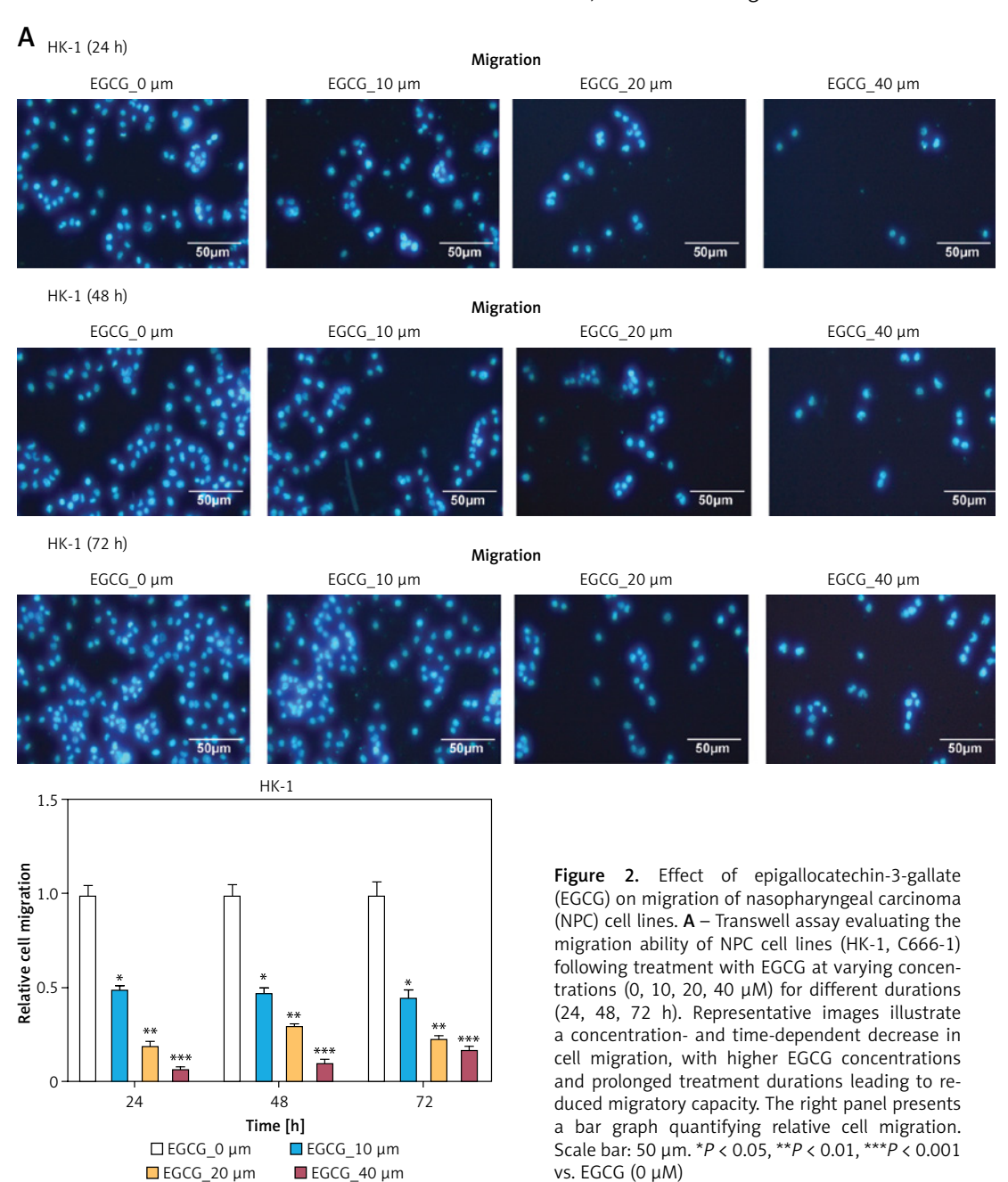


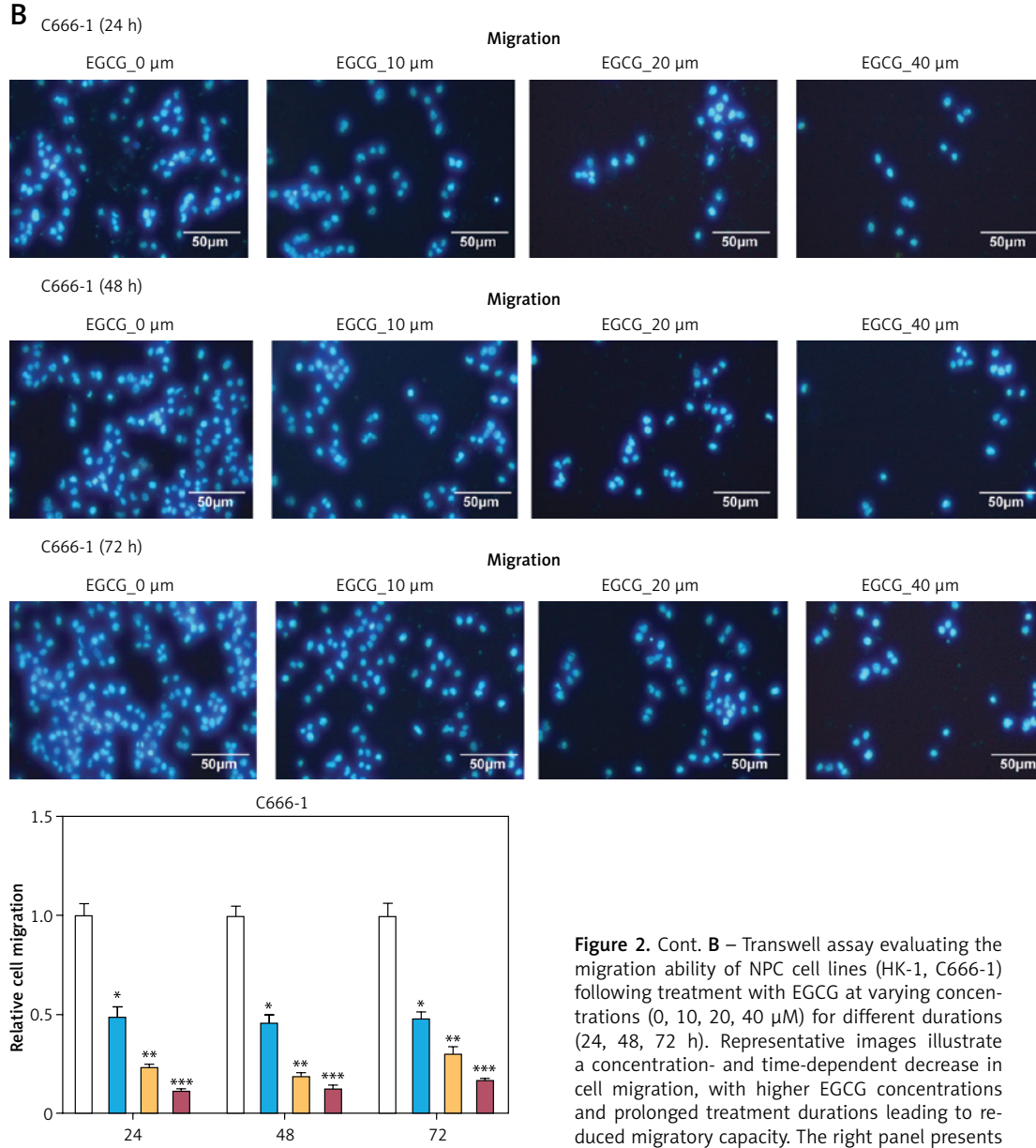
Figure 1. Effect of epigallocatechin-3-gallate (EGCG) on proliferation of nasopharyngeal carcinoma (NPC) cell lines. A, B – CCK-8 assay measuring cell viability of NPC cell lines (HK-1, C666-1) following treatment with increasing concentrations of EGCG (0, 10, 20, 40 μ M) for 48 hours. *P < 0.05, **P < 0.01 vs. EGCG (0 μ M). C, D – CCK-8 assay assessing cell viability of NPC cell lines (HK-1, C666-1) after exposure to 40 μ M EGCG for varying durations (0, 24, 48, 72 h). *P < 0.05, **P < 0.01 vs. EGCG (0 h). E, F – Cell Counting Kit-8 (CCK-8) assay evaluating the long-term effects of EGCG on NPC cell proliferation, with HK-1 and C666-1 cells treated with different concentrations of EGCG (0, 10, 20, 40 μ M) for extended periods (1, 3, 5, 7 days). *P < 0.05, **P < 0.01 vs. EGCG (0 μ M)

h to investigate the effects on the cell cycle and cell apoptosis. Flow cytometry showed that EGCG induced apoptosis in C666-1 and HK-1 cells in a dose-dependent manner (significant; Figures 3 A, B). In comparison with the control group, a significant elevation in apoptosis rates was observed at concentrations of 20 μM and 40 μM . In addition, cell cycle distribution analysis revealed that EGCG treatment resulted in G2 phase arrest in both cell lines, particularly at 40 μM , while the cells in the G1 phase declined accordingly (Figures 3 C, D). These results indicate that EGCG not only promotes apoptosis but also inhibits cell cycle progression by inducing G2 phase arrest in NPC cells.

DEGs identification and enrichment analysis of nasopharyngeal carcinomarelated datasets

263 upregulated DEGs and 445 downregulated DEGs were identified from the GSE12452 dataset, while 198 up-DEGs and 695 down-DEGs were obtained from the GSE64634 dataset (Figures 4 A, B). Cross-analysis of up-DEGs and down-DEGs from both datasets revealed 49 overlapping upregulated DEGs and 287 overlapping downregulated DEGs (Figure 4 C). The overlapping DEGs' enrichment study revealed a correlation with pathways such as the IL-17 signaling pathway, glycolysis/gluconeogenesis, and ferroptosis (Figure 4 D). Further investigation demonstrated that





DEGs were also significantly enriched in biological terms, including axoneme assembly, vesicle-related processes, and tubulin binding (Figure 4 E).

Time [h]

■ EGCG_10 µm

■ EGCG 40 µm

□ EGCG_0 μm

■ EGCG 20 µm

Identification and expression analysis of key genes

PPI network analysis was performed on the overlapping DEGs using the MCC and MCODE algorithms. The MCC algorithm identified a network comprising 10 nodes and 45 edges, whereas the MCODE algorithm revealed a network with 21 nodes and 207 edges (Figures 5 A, B). Cross-analysis of these two algorithms revealed 10 key genes: C5ORF49, CFAP126, CFAP45, CFAP52, EFHC1, EFHC2, ENKUR, PACRG,

a concentration- and time-dependent decrease in cell migration, with higher EGCG concentrations and prolonged treatment durations leading to reduced migratory capacity. The right panel presents a bar graph quantifying relative cell migration. Scale bar: $50 \, \mu m. *P < 0.05, **P < 0.01, ***P < 0.001 vs. EGCG (0 <math>\mu M$)

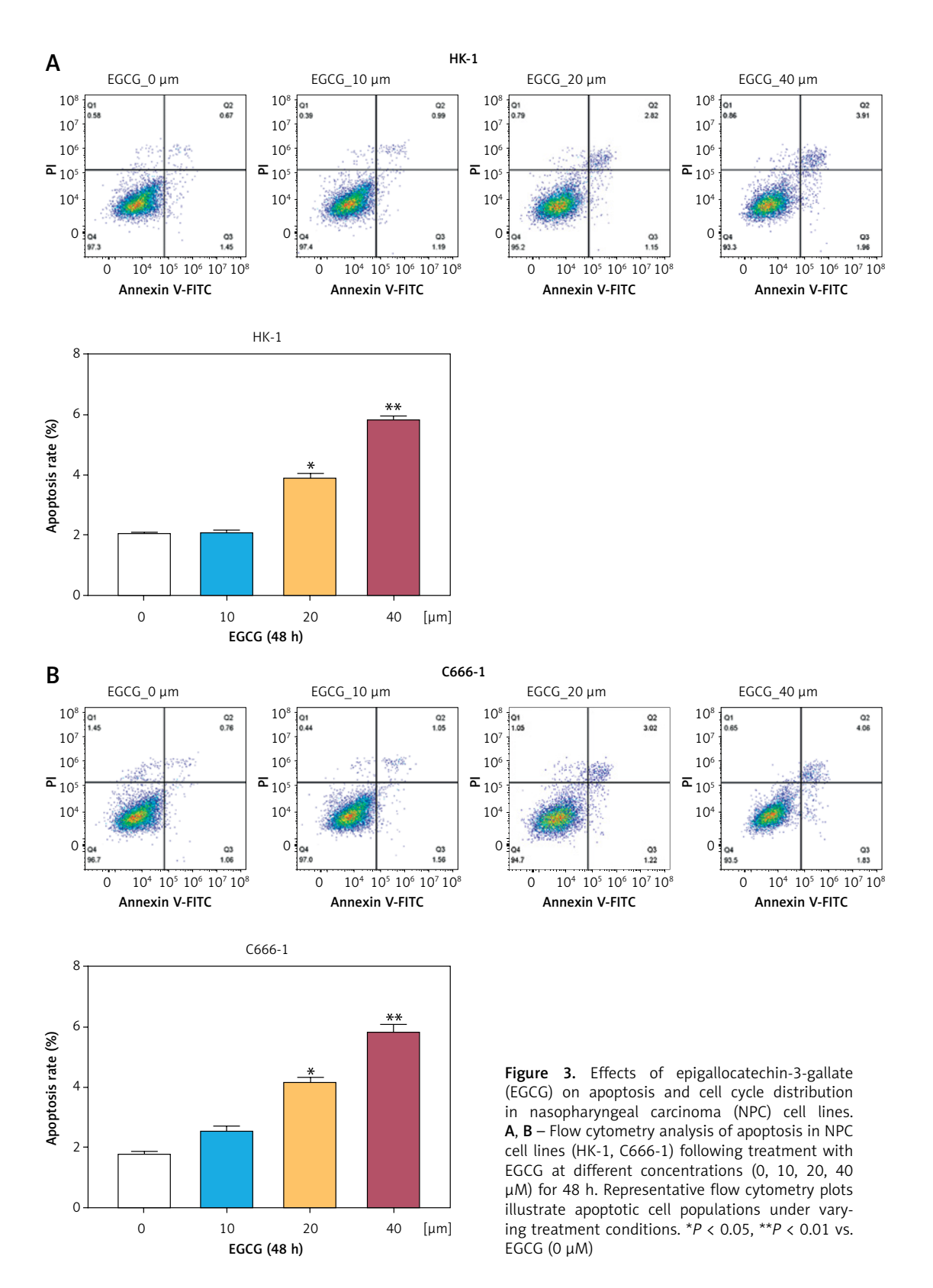
TEKT1, and TEKT2 (Figure 5 C). Expression analysis revealed that all ten key genes were downregulated in tumor samples from both the GSE12452 and GSE64634 datasets (Figures 5 D, E).

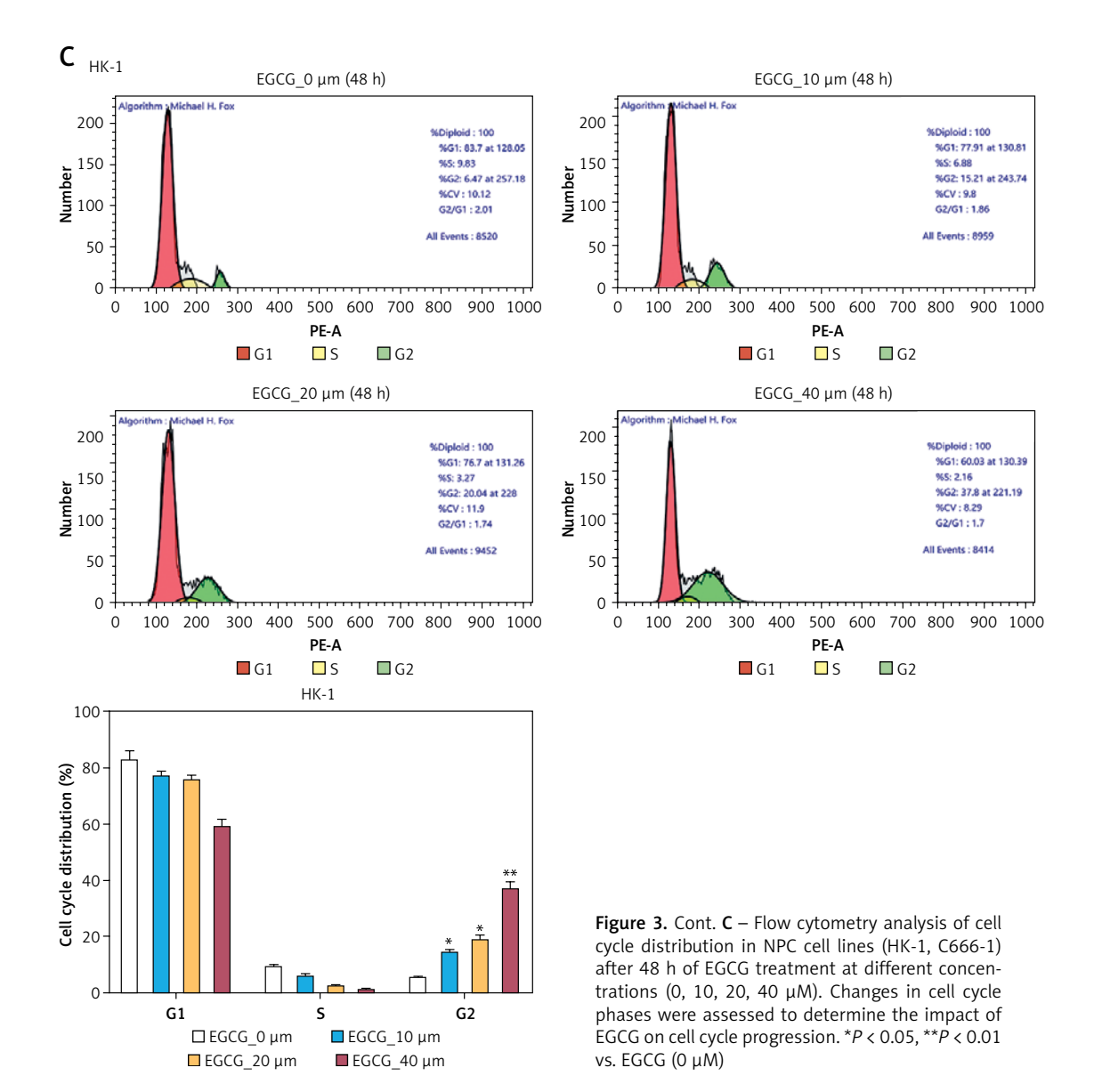
EGCG upregulates *PACRG* expression in NPC cells

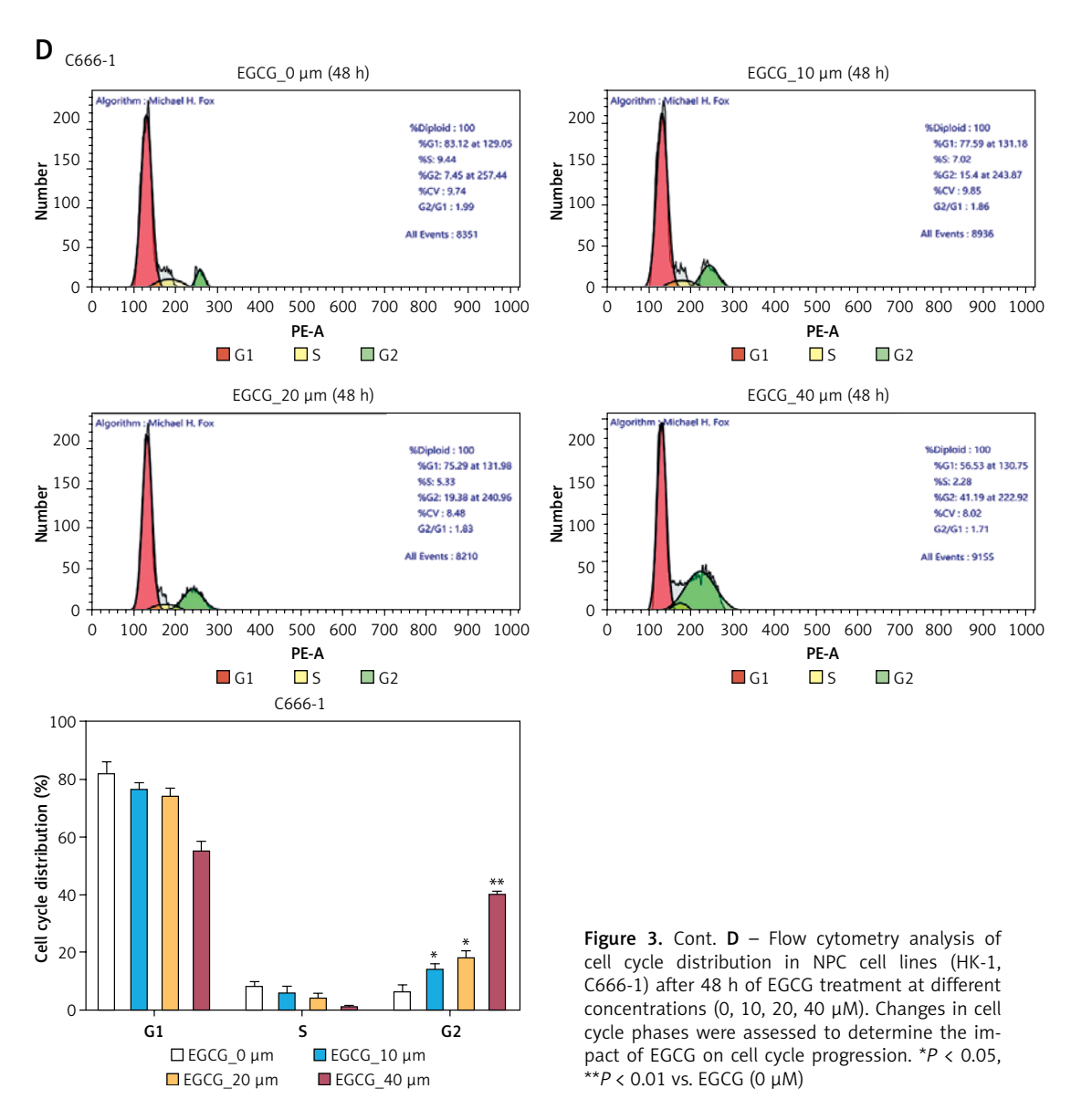
PACRG expression in NPC cell lines (HK-1 and C666-1) and NP69 cells was evaluated by qRT-PCR and WB analyses. The outcomes demonstrated significantly lower *PACRG* expression in HK-1 and C666-1 cells compared to NP69 cells (Figures 6 A–C). Next, we explored whether EGCG affects the level of *PACRG* in NPC cells. Treatment with

increasing EGCG concentrations (0, 10, 20, and 40 μ M) significantly increased the *PACRG* mRNA levels in C666-1 cells and HK-1 cells in a concentration-dependent manner (Figures 6 D, E). WB

analysis also revealed that the PACRG protein expression was upregulated after EGCG treatment (Figures 6 F–I), confirming the regulation of PACRG expression by EGCG.





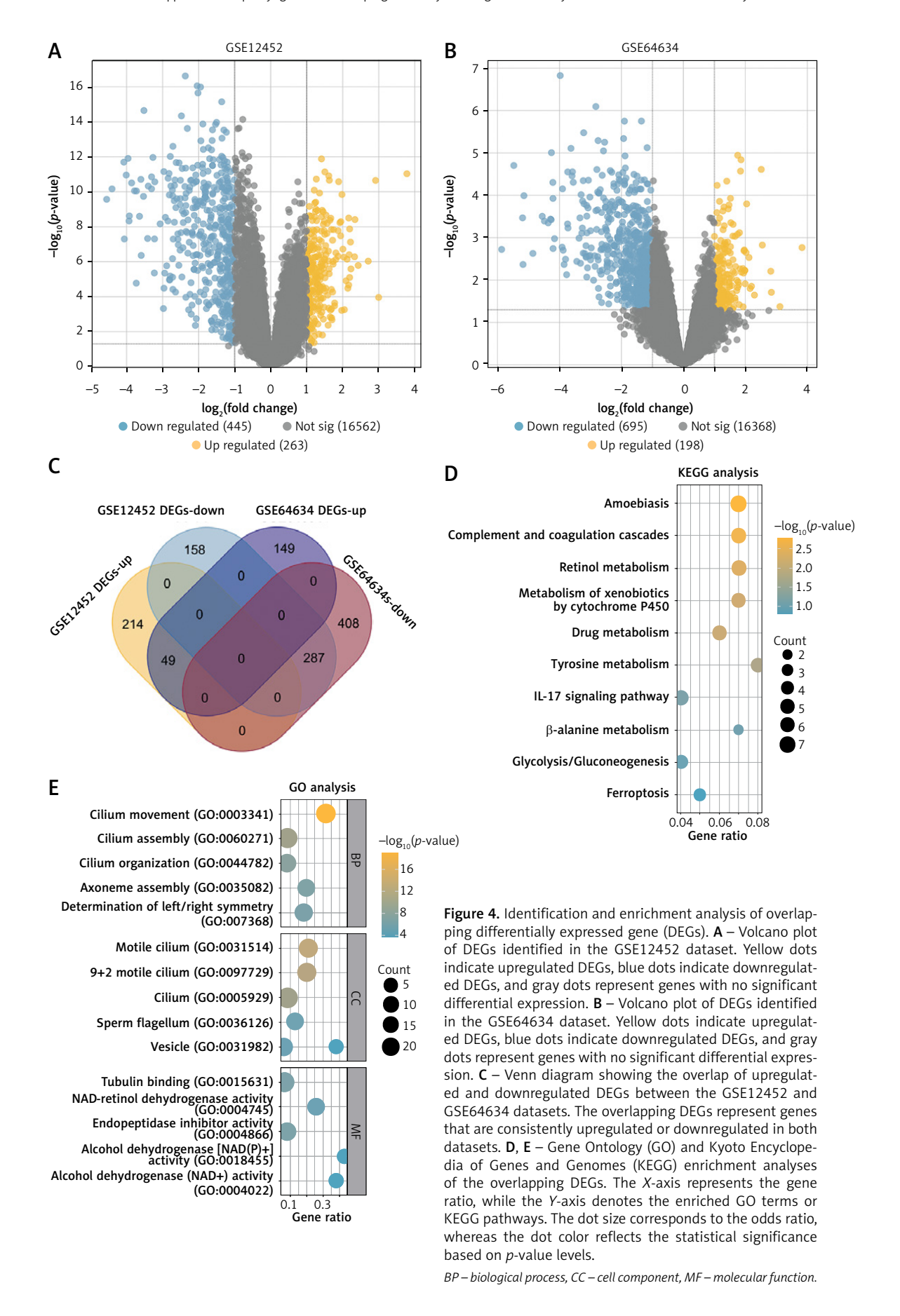


PACRG silencing reverses the inhibitory effect of EGCG on NPC cell function

qRT-PCR and WB analyses verified the effective PACRG knockdown in HK-1 and C666-1 cells, with si-PACRG-2 exhibiting the highest silencing efficiency. Therefore, si-PACRG-2 was selected for subsequent experiments (Figures 7 A-C). Functionally, PACRG knockdown significantly reversed the EGCG-induced attenuation in cell viability (Figures 7 D, E). Similarly, EGCG-mediated inhibition of cell proliferation was rescued considerably by PACRG knockdown (Figures 7 F, G). In addition, Transwell migration assays showed that PACRG knockdown restored the migration ability of NPC cells treated with EGCG (Figure 7 H). Quantitative analysis data showed that there were more migratory cells in the EGCG + si-PACRG-2 group than in the EGCG + si-NC group. These outcomes imply that PACRG is functionally involved in mediating the antiproliferative and antimigratory effects of EGCG in NPC cells.

PACRG silencing partially reverses EGCGinduced apoptosis and cell cycle G2 arrest in NPC cells

Flow cytometry analysis was used to assess apoptosis and cell cycle distribution in NPC cells treated with 40 μ M EGCG and si-*PACRG*-2 for 48 h. The results indicated that *PACRG* knockdown significantly reduced EGCG-induced apoptosis (Figures 8 A, B). Furthermore, EGCG treatment resulted in G2 phase arrest, thereby increasing the number of cells in the G2 phase. *PACRG* knockdown partially reversed this effect, reducing the percentage of G2-arrested cells (Figures 8 C, D). These findings suggest that EGCG promotes NPC cell apoptosis and G2 arrest, at least in part, by upregulating *PACRG*.



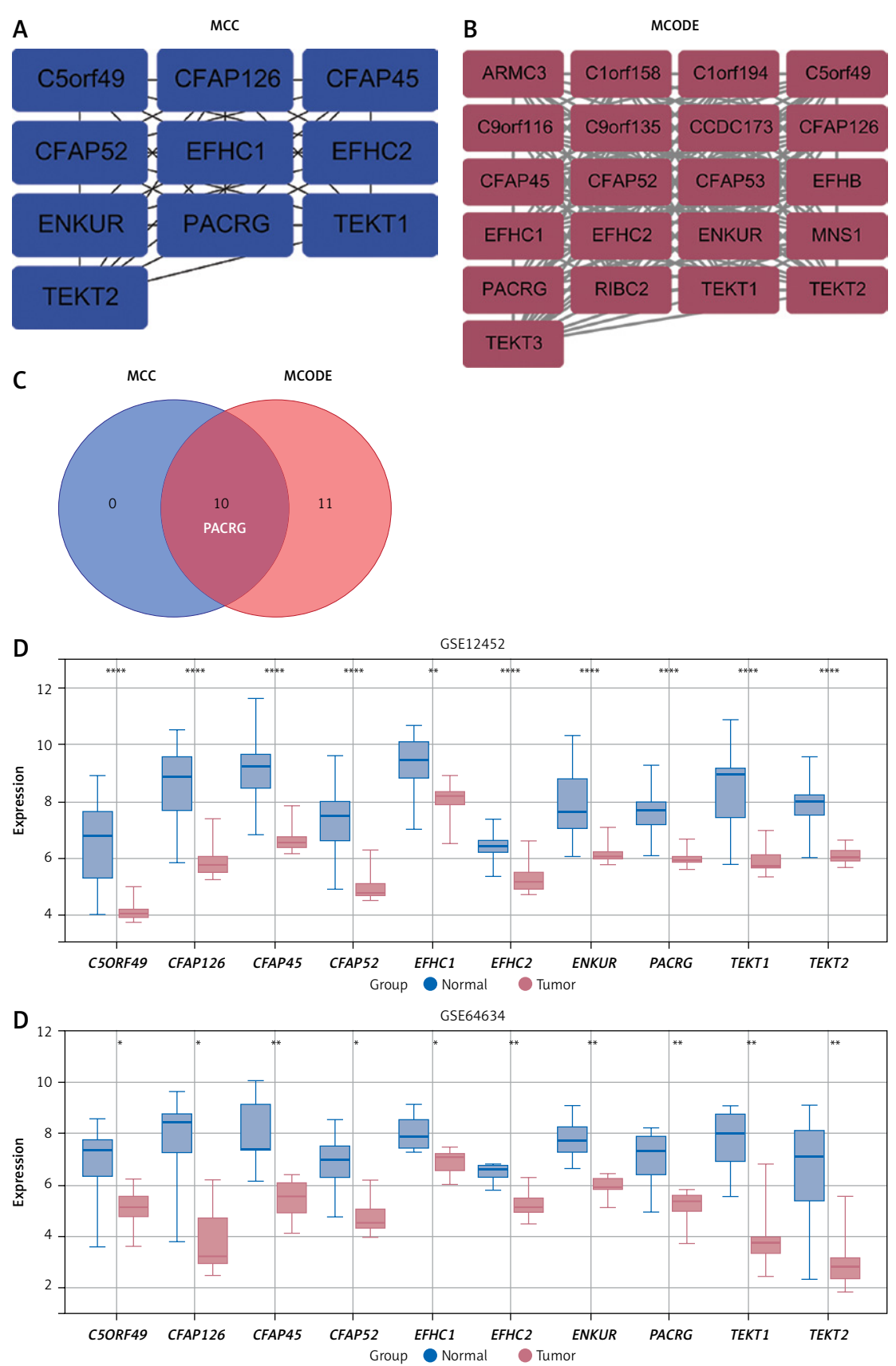


Figure 5. Identification and expression analysis of key genes. A, B – Protein-protein interaction (PPI) network analysis of overlapping differentially expressed genes (DEGs) using the Maximal Clique Centrality (MCC) and Molecular Complex Detection (MCODE) algorithms. The MCC algorithm identified a subnetwork consisting of 10 nodes and 45 edges, while the MCODE algorithm revealed a subnetwork comprising 21 nodes and 207 edges. C – Cross-analysis of the MCC and MCODE results identified 10 key genes: C5ORF49, CFAP126, CFAP45, CFAP52, EFHC1, EFHC2, ENKUR, PACRG, TEKT1, and TEKT2. D, E – Expression analysis of the 10 key genes in tumor and normal samples from the GSE12452 and GSE64634 datasets. The box plots display the expression levels of these genes, with blue representing normal tissue samples and red representing tumor samples. *P < 0.05, **P < 0.01, ****P < 0.0001 vs. normal

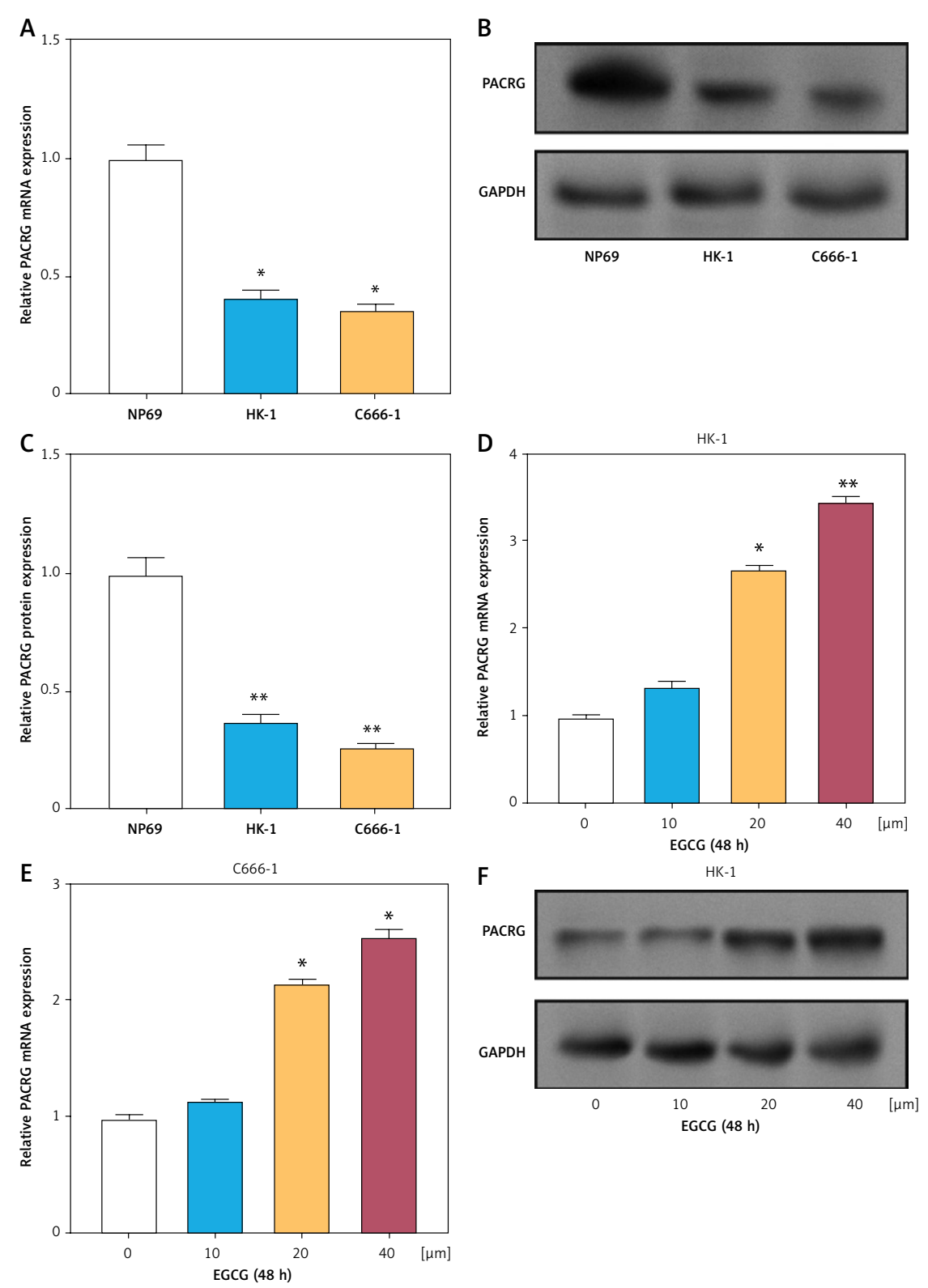
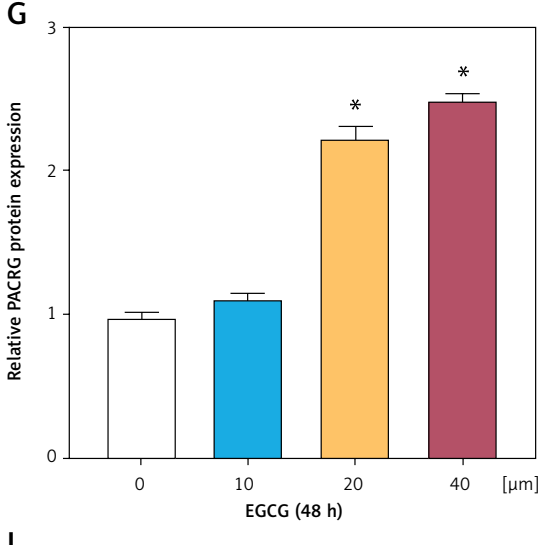
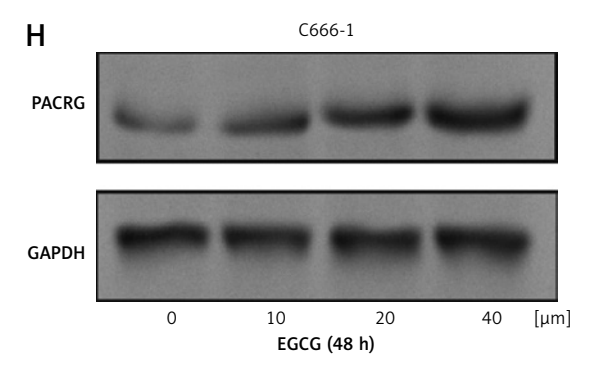


Figure 6. Epigallocatechin-3-gallate (EGCG) promotes expression of *PACRG* in nasopharyngeal carcinoma (NPC) cell lines. **A** – Quantitative real-time polymerase chain reaction (qRT-PCR) analysis of *PACRG* mRNA xpression in the human nasopharyngeal epithelial cell line NP69 and the NPC cell lines HK-1 and C666-1. * * P < 0.05 vs. NP69. **B**, **C** – Western blot (WB) analysis of PACRG protein expression in NP69, HK-1, and C666-1 cell lines. **C** – Grayscale quantification of WB results. * * P < 0.01 vs. NP69. **D**, **E** – qRT-PCR analysis of *PACRG* mRNA expression in HK-1 and C666-1 cell lines treated with different concentrations of EGCG (0, 10, 20, 40 μM) for 48 h. * * P < 0.05, * * P < 0.01 vs. EGCG (0 μM). **F** – WB analysis of PACRG protein expression in HK-1 and C666-1 cell lines following treatment with increasing EGCG concentrations (0, 10, 20, 40 μM) for 48 h. * * P < 0.05 vs. EGCG (0 μM)





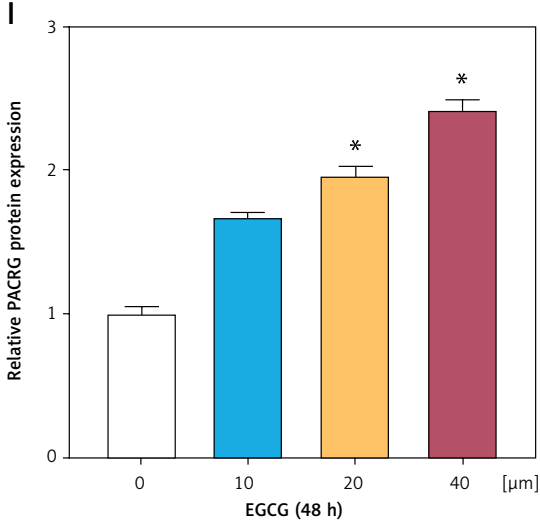


Figure 6. Cont. G–I – WB analysis of PACRG protein expression in HK-1 and C666-1 cell lines following treatment with increasing EGCG concentrations (0, 10, 20, 40 μ M) for 48 h. G and I – Grayscale quantification of WB results. *P < 0.05 vs. EGCG (0 μ M)

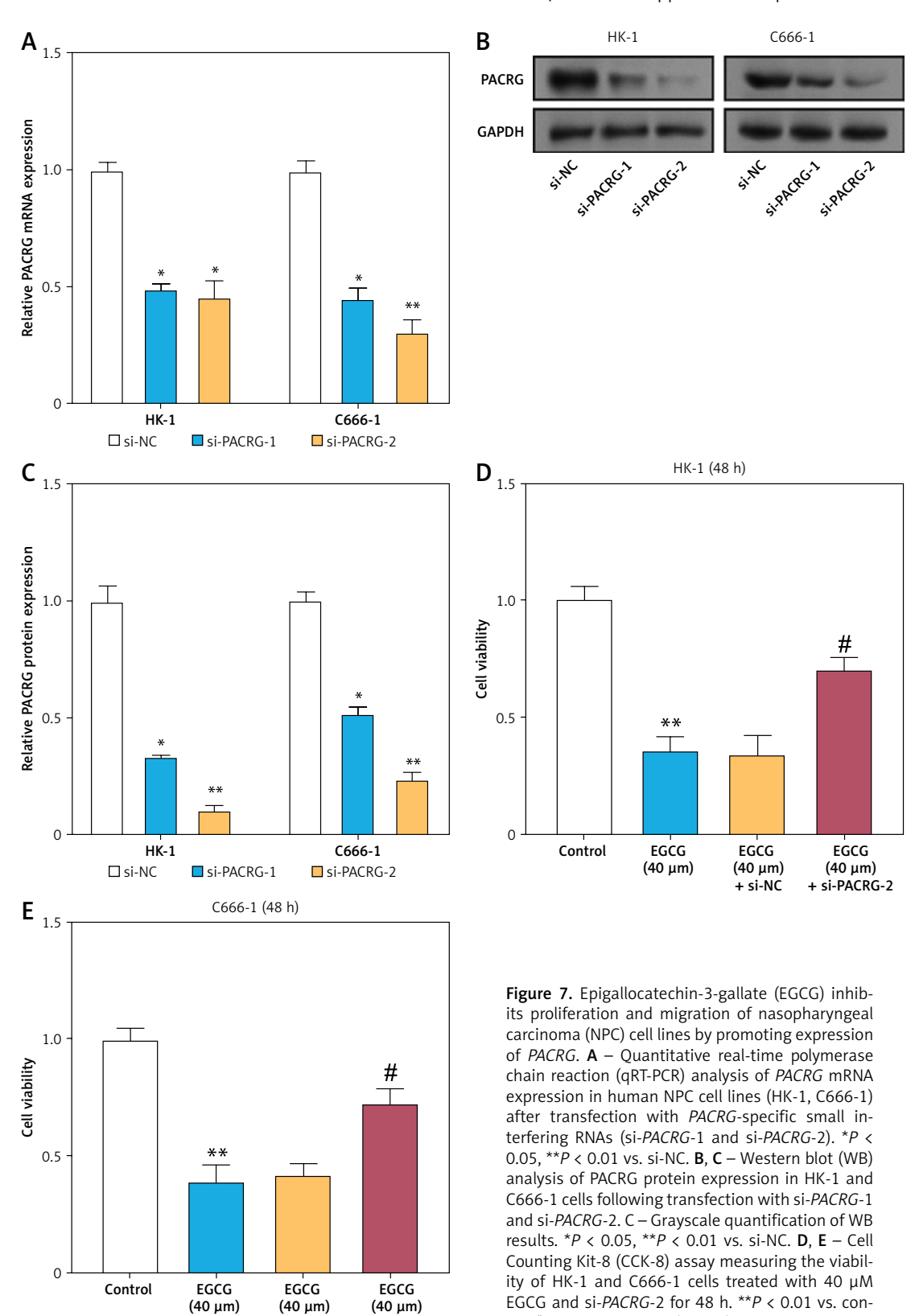
EGCG affects the methylation level of the *PACRG* promoter by reducing DNA methyltransferase in NPC cell lines

To investigate whether PACRG is regulated by epigenetic silencing in NPC cells, we first used MSP to detect the methylation status of its promoter region. As shown in Figure 9 A, NPC cell lines HK-1 and C666-1 both exhibited significant PACRG methylation bands, indicating that their promoter region is highly methylated. Subsequently, RT-PCR analysis revealed that PACRG mRNA expression was significantly downregulated in NPC cells (Figure 9 B), suggesting that its silencing may be closely related to high methylation of the promoter. To assess whether EGCG could reverse this methylation state, HK-1 and C666-1 cells were treated with 40 μ M EGCG or 5 μ M DNA methyltransferase inhibitor 5-aza-dC for 48 h. The MSP results (Figures 9 C, D) showed that the methylation bands of PACRG weakened while the unmethylated bands were enhanced, indicating that EGCG can induce demethylation of the PACRG promoter. Further analysis showed that treatment with both EGCG and 5-aza-dC led to an increase in 5-hydroxymethylcytosine (5hmC) levels and a decrease in 5-methylcytosine (5mC) levels (Figure 9 E), suggesting that these treatments reduce overall DNA methylation. RT-PCR results also showed that both EGCG and 5-aza-dC significantly restored PACRG mRNA expression (Figure 9 F), further supporting that they relieve the epigenetic silencing of PACRG through demethylation mechanisms. Additionally, qRT-PCR analysis indicated that EGCG significantly downregulated the mRNA expression of DNMT1, DNMT3A, and DNMT3B (Figures 9 G, H). Further enzyme activity assays (Figures 9 I, J) revealed that EGCG also inhibited the enzyme activity of these three DNMTs, showing effects similar to those of 5-azadC. In summary, EGCG may restore PACRG expression and exert its anti-cancer effects by inhibiting the expression and activity of DNMTs, thereby reducing DNA methylation levels.

EGCG inhibits NPC progression by reducing the methylation level of *PACRG*

To determine whether the demethylation and reactivation of *PACRG* contribute to the anti-tu-

mor impacts of EGCG, functional assays were conducted in NPC cell lines. As illustrated in Figures 10 A and B, CCK-8 assays revealed that treatment with 40 μ M EGCG suppressed the proliferation of

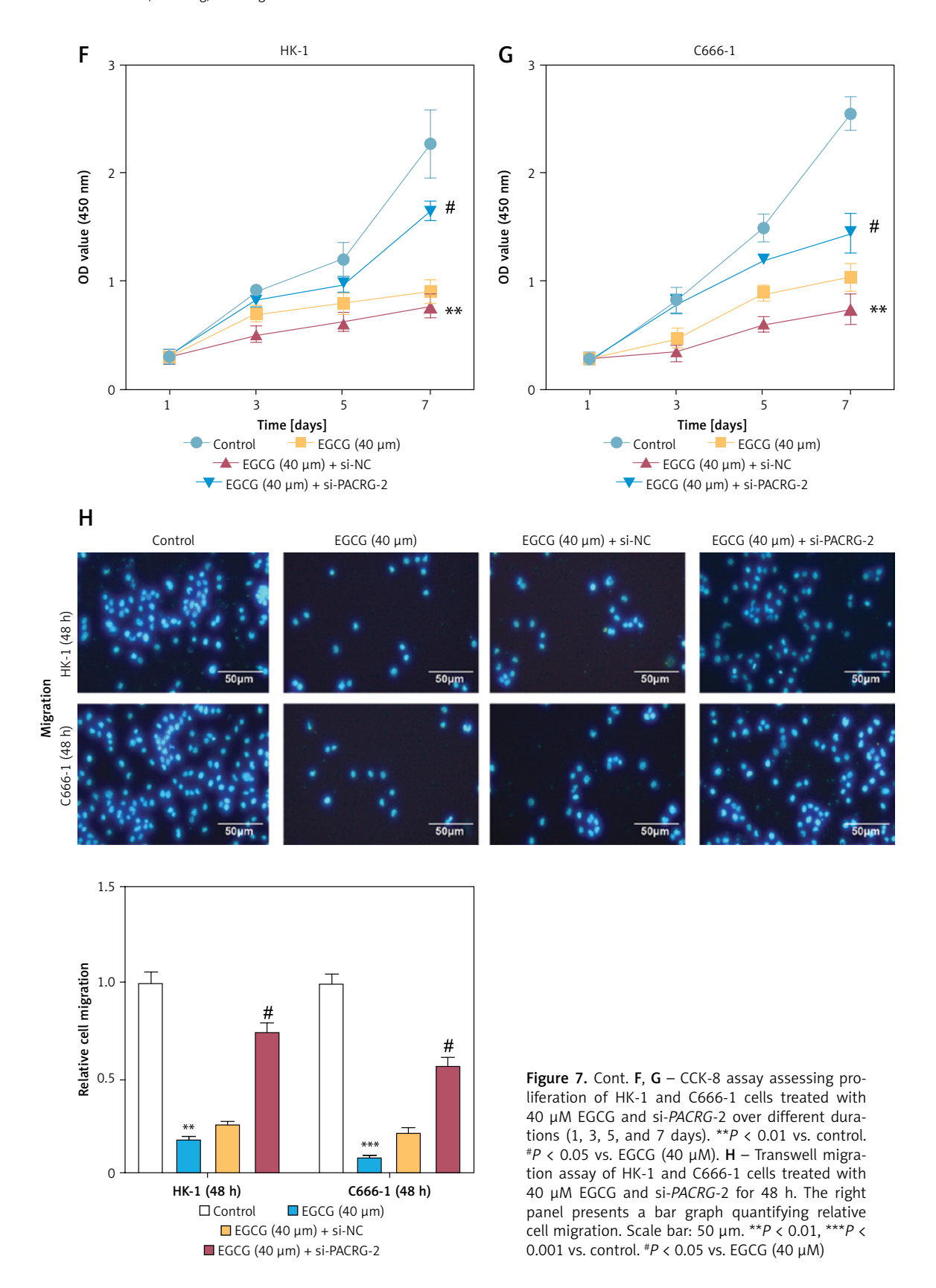


Arch Med Sci 15

+ si-PACRG-2

+ si-NC

trol. $^{\#}P$ < 0.05 vs. EGCG (40 μ M)

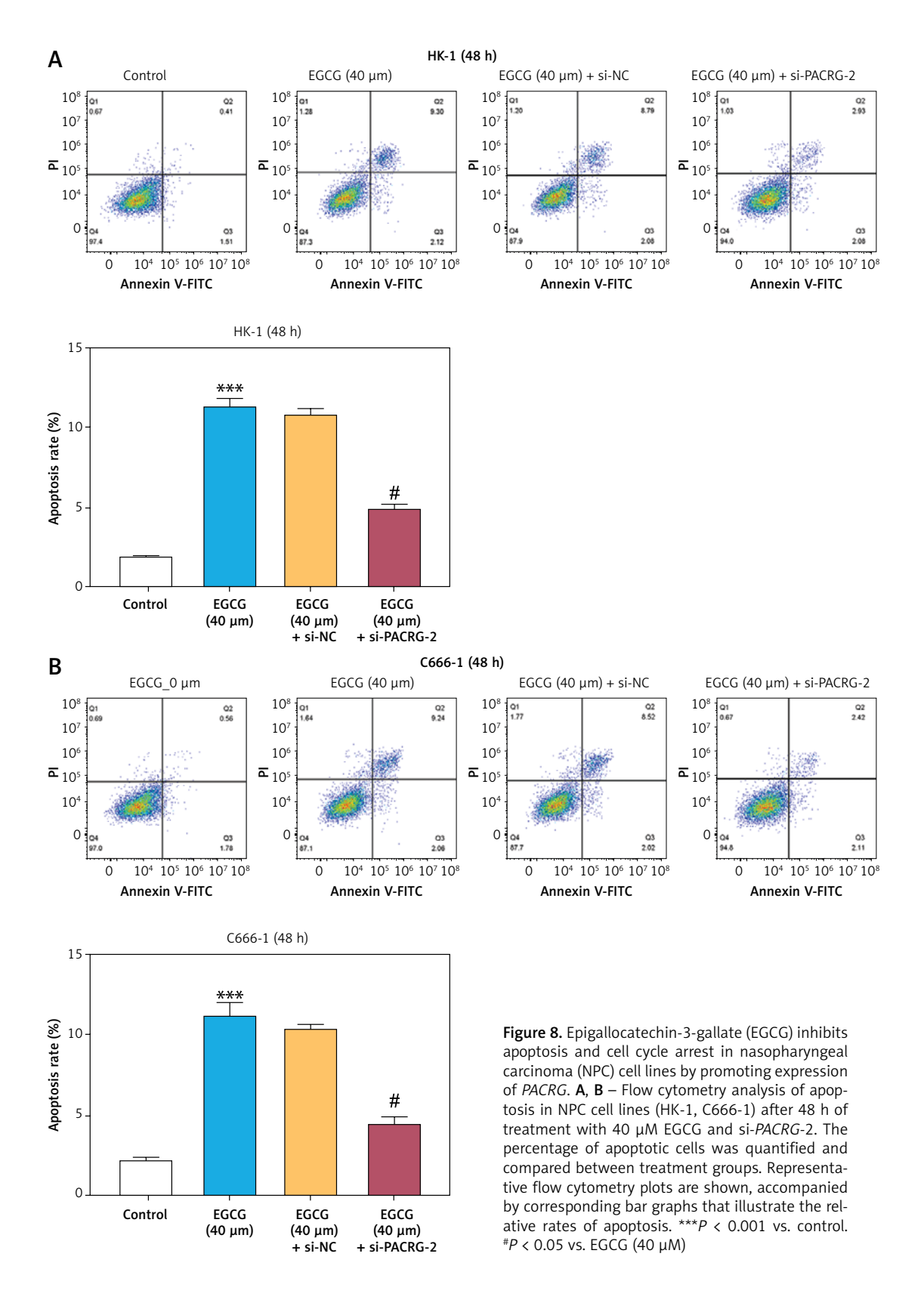


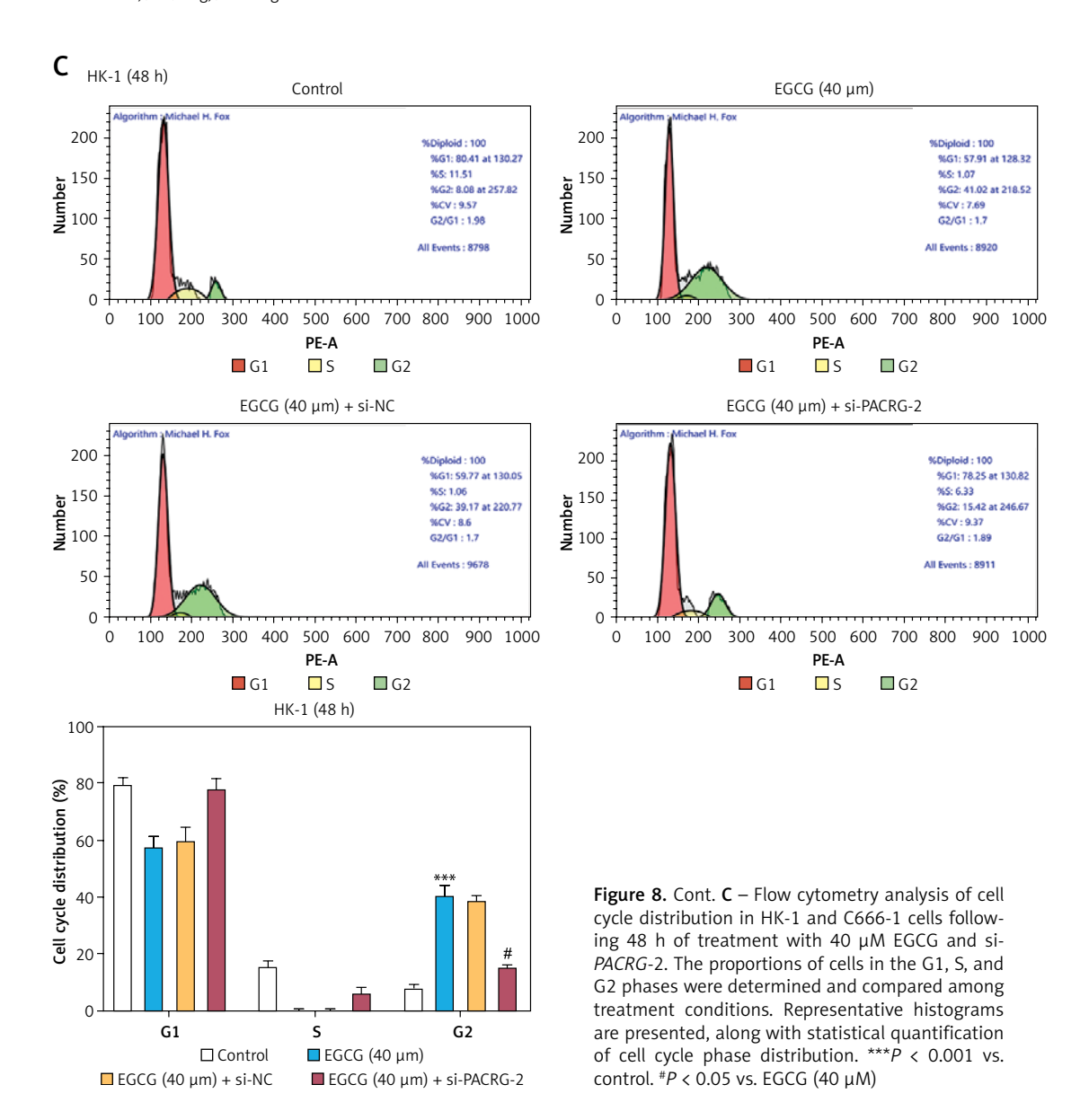
HK-1 and C666-1 cells compared to the untreated control. Similar effects were observed with 5 μ M 5-aza-dC, suggesting that demethylation mechanisms may mediate the suppression of NPC

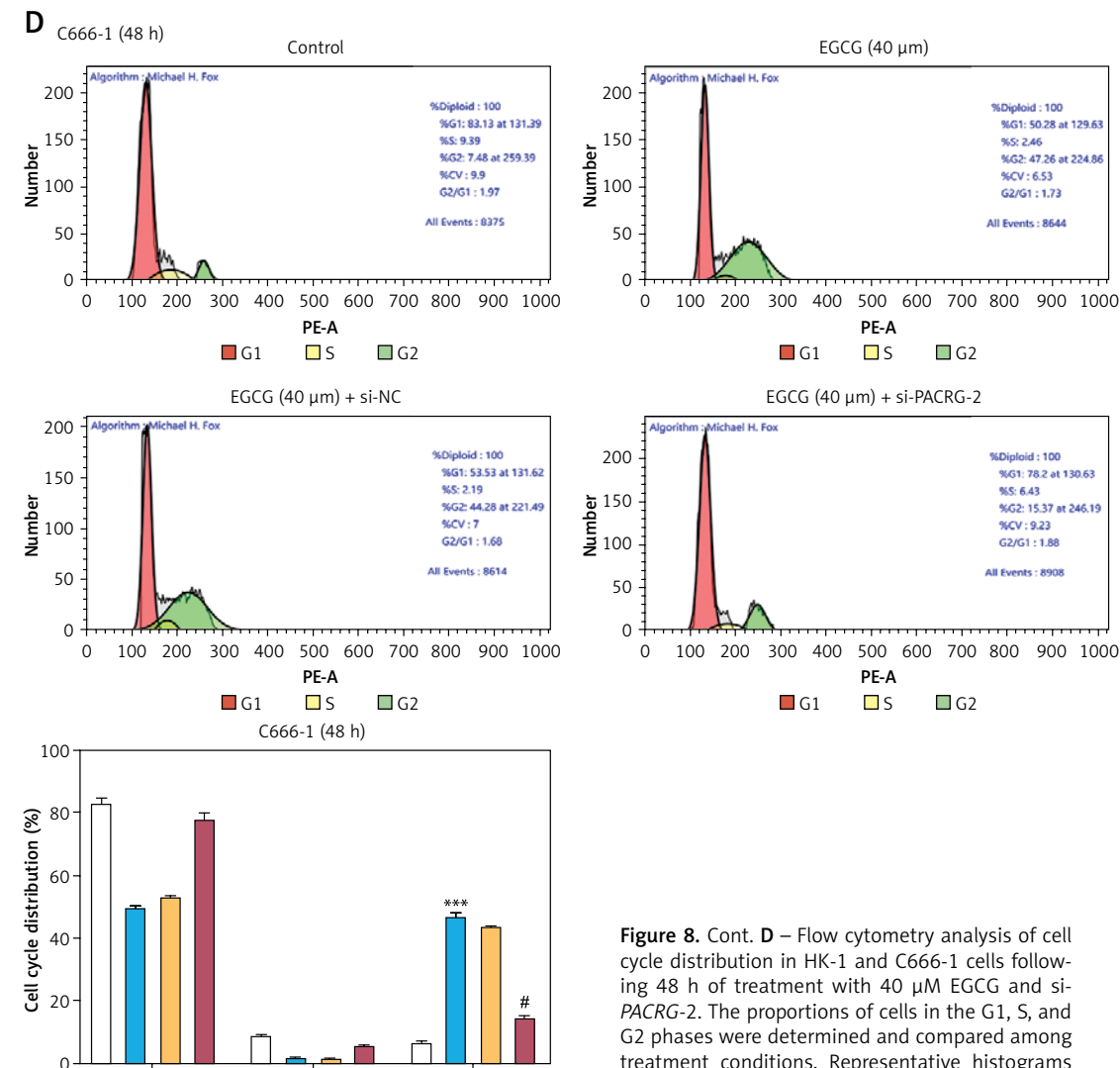
cell growth by EGCG. Transwell migration assays demonstrated that both EGCG and 5-aza-dC reduced the migratory capacity of NPC cells (Figure 10 C). Furthermore, flow cytometry analysis indi-

cated that EGCG and 5-aza-dC both induced significant apoptosis in C666-1 and HK-1 cells after 48 h of treatment (Figure 10 D). Together with our previous findings that EGCG reduces *PACRG*

promoter methylation and restores its expression, these functional results suggest that EGCG suppresses NPC progression, at least in part, by epigenetically reactivating *PACRG*.







Discussion

G1

■ EGCG (40 μm) + si-NC

☐ Control

■ EGCG (40 μm)

■ EGCG (40 µm) + si-PACRG-2

EGCG, the most abundant catechin in green tea, has been widely reported to exert anticancer effects by modulating apoptosis, cell cycle progression, and metastatic potential across various malignancies [7–9]. Consistent with previous findings in NPC, our study demonstrated that EGCG inhibits NPC cell viability, proliferation, and migration in a dose- and time-dependent manner [10-12]. In addition to reducing cell viability, EGCG impaired colony formation and significantly suppressed cell motility. Importantly, EGCG induced apoptosis and G2 cell cycle arrest, highlighting its potential to disrupt tumor growth through multiple biological processes [11, 16].

To further explore EGCG's mechanism of action, transcriptomic analyses were performed on two independent GEO datasets (GSE12452 and GSE64634). PACRG was identified among

treatment conditions. Representative histograms are presented, along with statistical quantification of cell cycle phase distribution. ***P < 0.001 vs. control. $^{\#}P$ < 0.05 vs. EGCG (40 μ M)

the downregulated genes in NPC tissues. While PACRG has been previously implicated in renal cell carcinoma and hematologic malignancies [19, 20], its role in NPC has not been reported. In our study, EGCG significantly upregulated PACRG expression in a concentration-dependent manner. Functional assays revealed that PACRG knockdown partially reversed the inhibitory effects of EGCG on proliferation and migration. They attenuated its pro-apoptotic and cell cycle-arresting effects, supporting PACRG's functional involvement in EGCG's antitumor action.

Epigenetic silencing via promoter hypermethylation is a common mechanism underlying the inactivation of tumor suppressor genes. DNA methylation is mediated by DNA methyltransferases (DNMTs), with DNMT1 responsible for maintenance methylation and DNMT3A/3B for de novo methylation [22, 23]. Prior studies have shown that EGCG modulates gene expression epigenetically by

inhibiting DNMTs and restoring the expression of silenced tumor suppressors [14, 15]. Consistently, we found that the *PACRG* promoter is hypermethylated in NPC cells, contributing to its transcriptional silencing. Treatment with EGCG significantly re-

duced promoter methylation and restored *PACRG* expression, a finding similar to that of the DNA methylation inhibitor 5-aza-dC [24].

Notably, EGCG treatment resulted in the downregulation of DNMT1, DNMT3A, and DNMT3B, indi-

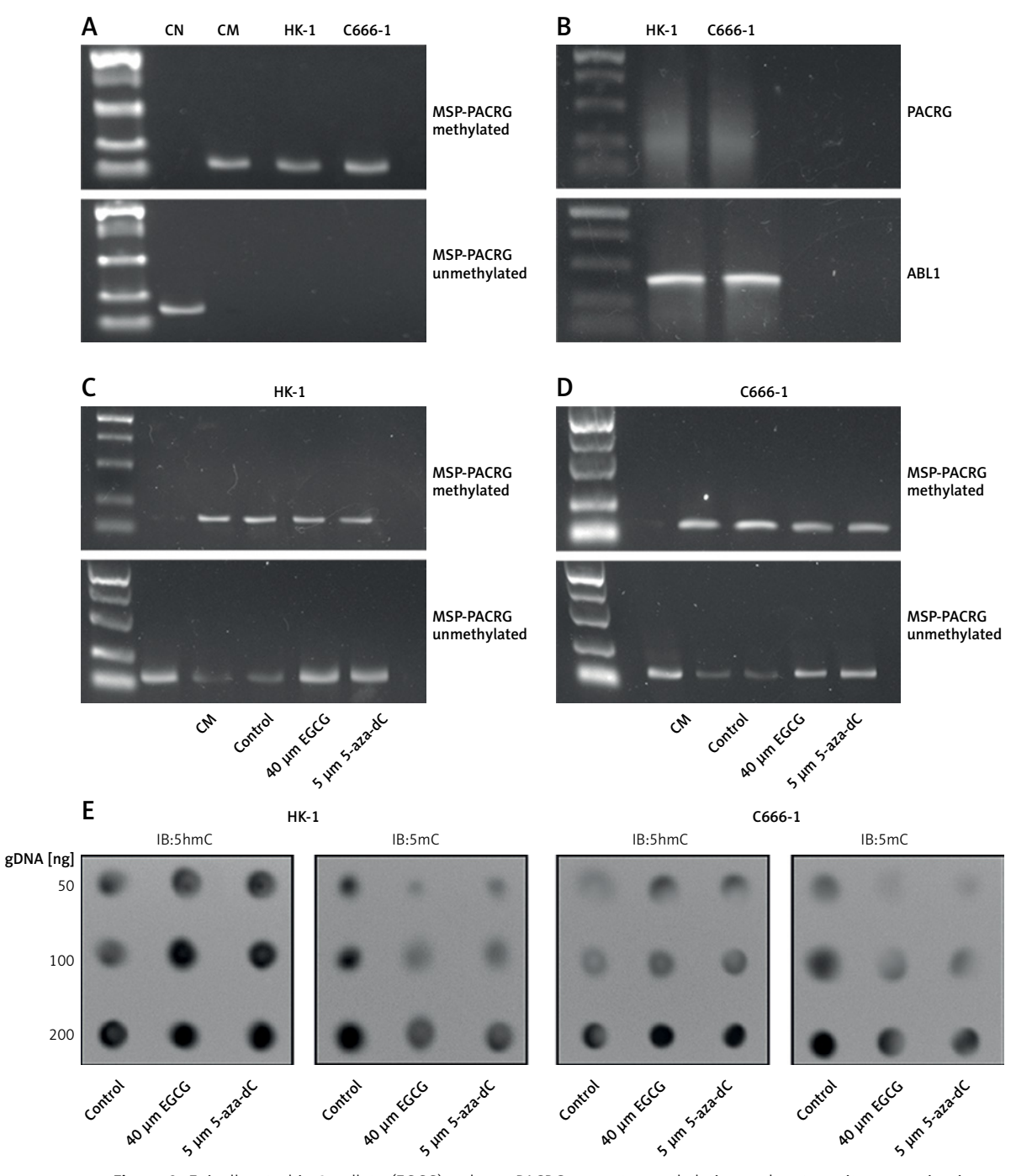
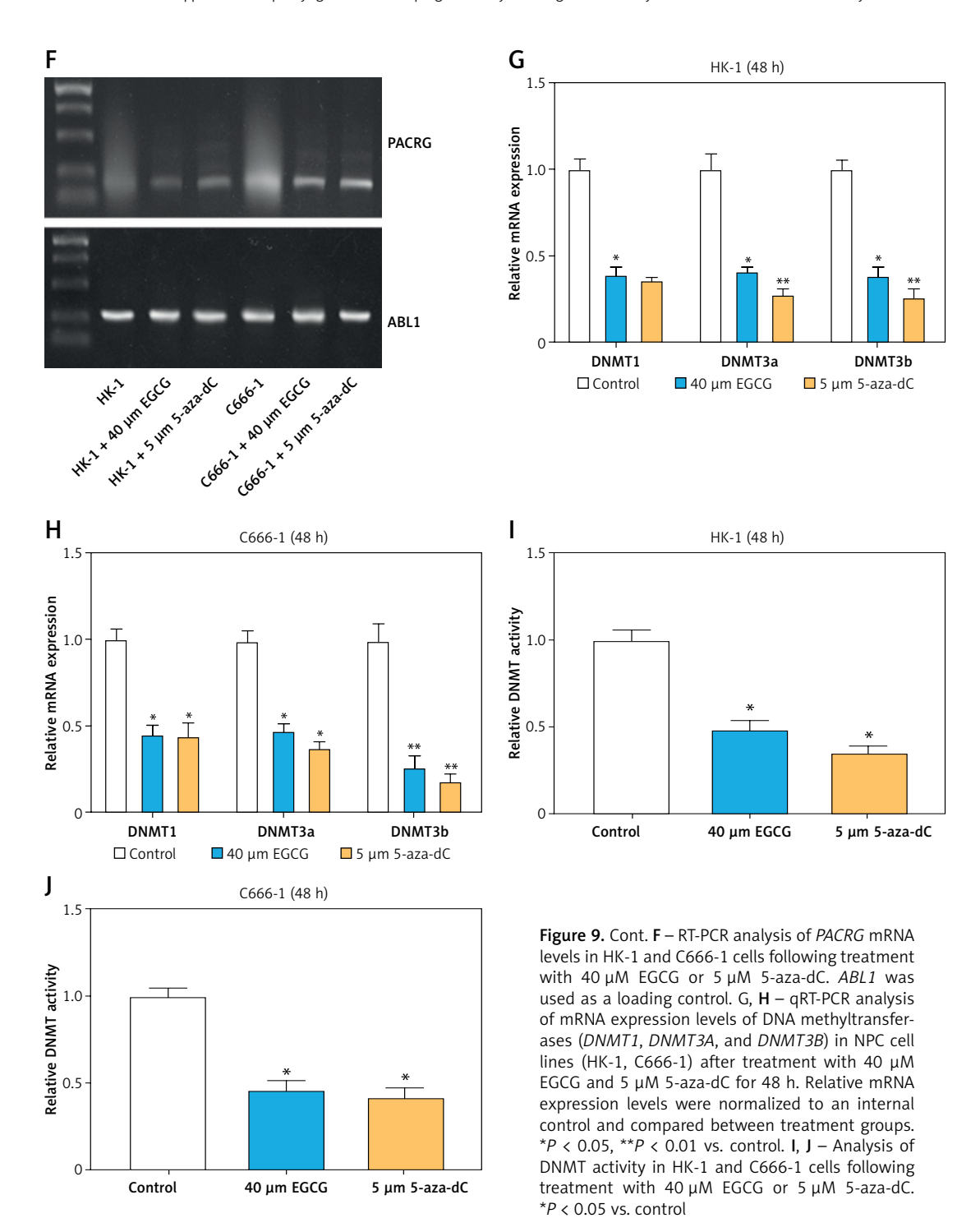
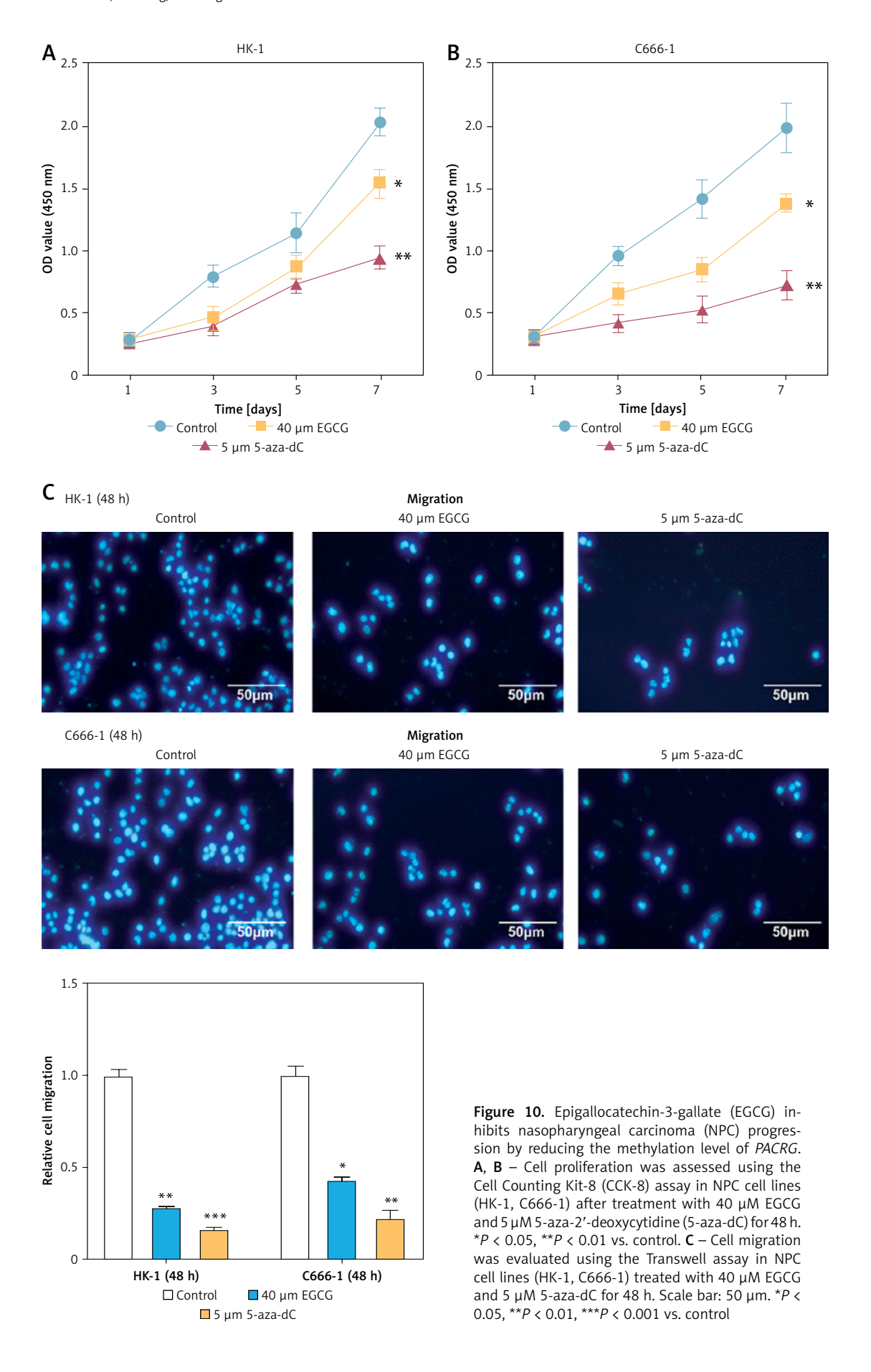


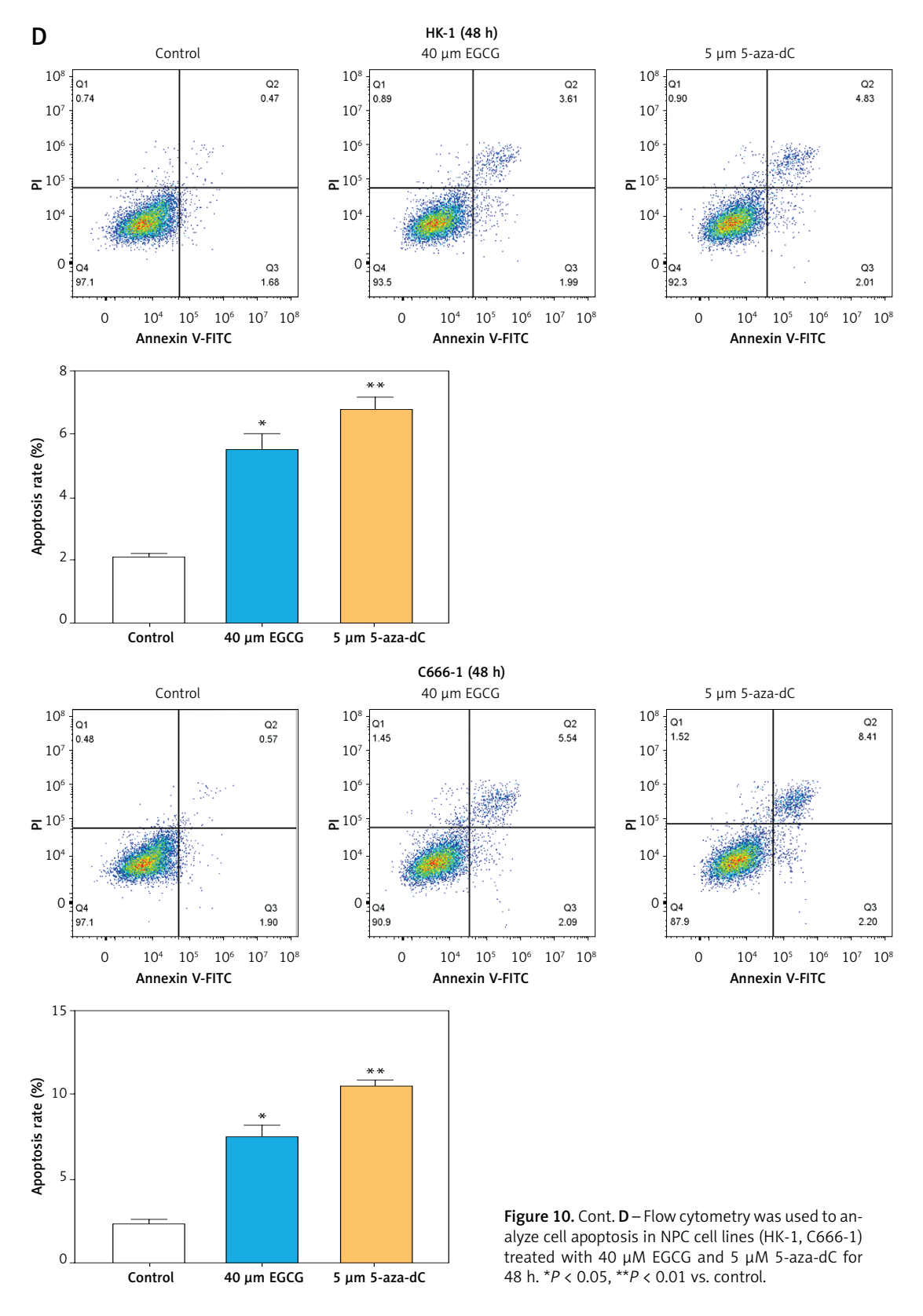
Figure 9. Epigallocatechin-3-gallate (EGCG) reduces *PACRG* promoter methylation and restores its expression in nasopharyngeal carcinoma (NPC) cells. **A** – Methylation-specific PCR (MSP) analysis of *PACRG* promoter methylation in HK-1 and C666-1 cells. CN (completely unmethylated control DNA) and CM (completely methylated control DNA) were used as positive controls for unmethylated and methylated PCR products, respectively. **B** – Semi-quantitative quantitative real-time polymerase chain reaction (RT-PCR) showing *PACRG* mRNA expression in HK-1 and C666-1 cells. *ABL1* was used as an internal control. **C**, **D** – MSP analysis of *PACRG* promoter in HK-1 cells treated with 40 μM EGCG or 5 μM 5-aza-2'-deoxycytidine (5-aza-dC) for 48 h. EGCG and 5-aza-dC both reduced methylated bands and increased unmethylated bands, indicating demethylation. **E** – Dot blot analysis was performed to assess global 5hmC and 5mC levels in HK-1 and C666-1 cells following treatment with 40 μM EGCG or 5 μM 5-aza-dC



cating that EGCG facilitates PACRG demethylation by inhibiting DNMTs. These findings are consistent with studies demonstrating that EGCG reduces methylation at specific promoter regions without altering global methylation, and reactivates silenced genes such as $RXR\alpha$ and PLAGL1 in other cancer types [13–15]. Functionally, both EGCG and 5-aza-dC similarly inhibited NPC cell proliferation and migration, and promoted apoptosis, reinforcing a demethylation-dependent mechanism underlying EGCG's anticancer activity in NPC.

While *PACRG* knockdown partially attenuated EGCG's effects, the incomplete reversal suggests that EGCG may target additional signaling molecules or pathways. Indeed, EGCG has been shown to regulate multiple cellular processes through different mechanisms, including SIRT1-p53 signaling, NF-kB inactivation, and modulation of miRNAs in NPC cells [10, 12, 25]. Our findings expand this mechanistic spectrum by implicating epigenetic reactivation of PACRG as a novel pathway by which EGCG suppresses NPC progression.





Although the concentrations used (10–40 μ M) exceed typical oral plasma levels, they are achievable via intravenous administration or nanoparticle-based delivery [26]. Importantly, EGCG exhibits selective cytotoxicity against NPC cells (TW01/NA)

compared to normal NP460hTert epithelial cells [11], indicating a favorable therapeutic index. Future studies will optimize dosing regimens to bridge this gap.

This study has several limitations. First, although *PACRG* was identified as a key mediator of

EGCG's antitumor effect, its downstream signaling pathways were not investigated and should be explored in future work. Second, while PACRG was the primary focus, EGCG is likely to affect additional methylation-regulated targets. Genome-wide methylation or transcriptomic profiling would help identify these. Third, methylation detection relied on MSP, which is semi-quantitative and may miss low-abundance events. Future studies employing targeted bisulfite next-generation sequencing (NGS) or digital PCR will enhance sensitivity and capture methylation heterogeneity, particularly in rare tumor subclones. Fourth, functional assays were limited to in vitro models. In vivo validation (e.g., xenografts, clinical samples) is necessary to confirm the therapeutic relevance and epigenetic role of PACRG in NPC. Fifth, we only performed a knockdown of PACRG. Overexpression studies are required to determine whether PACRG alone can suppress NPC growth. Lastly, PACRG knockdown only partially reversed the effects of EGCG, indicating that other targets or pathways may also contribute.

In conclusion, this investigation highlights the potential therapeutic effects of EGCG on NPC cells, demonstrating its ability to reduce cell viability, proliferation, and migration in a time- and dose-dependent manner. EGCG treatment also induced G2 phase cell cycle arrest and apoptosis, underscoring its role in inhibiting the growth of NPC cells. Furthermore, the upregulation of PACRG expression following EGCG treatment suggests its involvement in mediating these effects. Notably, PACRG knockdown partially reversed the EGCG-induced inhibition of proliferation, migration, and apoptosis, indicating its crucial role in EGCG's action. Additionally, EGCG was found to modulate the methylation status of the PACRG promoter by downregulating DNA methyltransferases, thereby contributing to the suppression of NPC progression. These outcomes highlight EGCG's potential as a novel therapeutic strategy for NPC treatment.

Funding

No external funding.

Ethical approval

Not applicable.

Conflict of interest

The authors declare no conflict of interest.

References

1. Wong KC, Hui EP, Lo KW, et al. Nasopharyngeal carcinoma: an evolving paradigm. Nat Rev Clin Oncol 2021; 18: 679-95.

- 2. Su ZY, Siak PY, Leong CO, Cheah SC. The role of Epstein–Barr virus in nasopharyngeal carcinoma. Front Microbiol 2023: 14: 1116143.
- 3. Stan D, Niculet E, Lungu M, et al. Nasopharyngeal carcinoma: a new synthesis of literature data. Exp Ther Med 2022; 23: 136.
- 4. Bayatfard P, Sari SY, Yazici G. Chemotherapy, radiation therapy, and nasopharyngeal carcinoma. JAMA Oncol 2024; 10: 1292.
- Zhang J, Tang H, Li H, Jiang D, Luo H. Case report of chemoradiotherapy combined with immunotherapy for liver metastasis and lymph node metastases in the head of the pancreas of nasopharyngeal carcinoma. Arch Med Sci 2022; 18: 1413-9.
- Song X, Wang S, Li J, Yan L, Chen F, Wang J. Induction chemotherapy plus nimotuzumab followed by concurrent chemoradiotherapy for advanced nasopharyngeal carcinoma. Arch Med Sci 2021; 17: 1317-24.
- 7. Wang S, Li Z, Ma Y, et al. Immunomodulatory effects of green tea polyphenols. Molecules 2021; 26: 3755.
- Ferrari E, Bettuzzi S, Naponelli V. The potential of epigallocatechin gallate (EGCG) in targeting autophagy for cancer treatment: a narrative review. Int J Mol Sci 2022; 23: 6075.
- Khiewkamrop P, Surangkul D, Srikummool M, et al. Epigallocatechin gallate triggers apoptosis by suppressing de novo lipogenesis in colorectal carcinoma cells. FEBS Open Bio 2022; 12: 937-58.
- 10. Jiang S, Huang C, Zheng G, et al. EGCG inhibits proliferation and induces apoptosis through downregulation of SIRT1 in nasopharyngeal carcinoma cells. Front Nutr 2022; 9: 851972.
- 11. Fang CY, Wu CC, Hsu HY, et al. EGCG inhibits proliferation, invasiveness and tumor growth by up-regulation of adhesion molecules, suppression of gelatinases activity, and induction of apoptosis in nasopharyngeal carcinoma cells. Int J Mol Sci 2015; 16: 2530-58.
- 12. Li YJ, Wu SL, Lu SM, et al. (-)-Epigallocatechin-3-gallate inhibits nasopharyngeal cancer stem cell self-renewal and migration and reverses the epithelial–mesenchymal transition via NF-κB p65 inactivation. Tumor Biol 2015; 36: 2747-61.
- 13. He C, Zhou J, Wang D, Wang R, Wu M, Dong T. PLAGL1 gene demethylation induced by epigallocatechin gallate promotes pheochromocytoma cell apoptosis via Wnt/β-catenin signaling pathway. Asian Pac J Cancer Prev 2022; 23: 2119-25.
- 14. Morris J, Moseley VR, Cabang AB, et al. Reduction in promotor methylation utilizing EGCG (epigallocate-chin-3-gallate) restores RXRα expression in human colon cancer cells. Oncotarget 2016; 7: 35313.
- 15. Agarwal A, Kansal V, Farooqi H, Prasad R, Singh VK. Epigallocatechin gallate (EGCG), an active phenolic compound of green tea, inhibits tumor growth of head and neck cancer cells by targeting DNA hypermethylation. Biomedicines 2023; 11: 789.
- Zhang W, Yang P, Gao F, Yang J, Yao K. Effects of epigallocatechin gallate on the proliferation and apoptosis of the nasopharyngeal carcinoma cell line CNE2. Exp Ther Med 2014; 8: 1783-8.
- 17. Zhang L, Rong W, Ma J, et al. Comprehensive analysis of DNA 5-methylcytosine and N6-adenine methylation by nanopore sequencing in hepatocellular carcinoma. Front Cell Devel Biol 2022; 10: 827391.
- 18. Han B, Yang X, Zhang P, et al. DNA methylation biomarkers for nasopharyngeal carcinoma. PLoS One 2020; 15: e0230524.

- 19. Toma MI, Wuttig D, Kaiser S, et al. PARK2 and PACRG are commonly downregulated in clear cell renal cell carcinoma and are associated with aggressive disease and poor clinical outcome. Genes Chromosomes Cancer 2013; 52: 265-73.
- 20. Agirre X, Román Gómez J, Vázquez I, et al. Abnormal methylation of the common PARK2 and PACRG promoter is associated with downregulation of gene expression in acute lymphoblastic leukemia and chronic myeloid leukemia. Int J Cancer 2006; 118: 1945-53.
- 21. Noël A, Ghosh A. Carbonyl profiles of Electronic Nicotine Delivery System (ENDS) aerosols reflect both the chemical composition and the numbers of E-Liquid ingredients-focus on the in vitro toxicity of strawberry and vanilla flavors. Int J Environ Res Public Health 2022; 19: 16774.
- Kafetzopoulos I, Taglini F, Davidson-Smith H, Sproul D. DNMT1 loss leads to hypermethylation of a subset of late replicating domains by DNMT3A. bioRxiv 2024: 2024.12.19.629414.
- Lauria A, Meng G, Proserpio V, et al. DNMT3B supports meso-endoderm differentiation from mouse embryonic stem cells. Nat Commun 2023; 14: 367.
- 24. Araki T, Hamada K, Myat AB, et al. Enhanced cytotoxicity on cancer cells by combinational treatment of PARP inhibitor and 5-azadeoxycytidine accompanying distinct transcriptional profiles. Cancers 2022; 14: 4171.
- 25. Li BB, Huang GL, Li HH, Kong X, He ZW. Epigallocatechin-3-gallate modulates microrna expression profiles in human nasopharyngeal carcinoma CNE2 cells. Chin Med J 2017; 130: 93-9.
- 26. Ramesh N, Mandal AKA. Encapsulation of epigallocatechin-3-gallate into albumin nanoparticles improves pharmacokinetic and bioavailability in rat model. 3 Biotech 2019; 9: 238.